Science of the Total Environment 835 (2022) 155434

Contents lists available at ScienceDirect

Science of the Total Environment

journal homepage: www.elsevier.com/locate/scitotenv

Distribution of microplastics in benthic sediments of Qinghai Lake on the Tibetan Plateau, China

Ning Jiang [a,b], Wei Luo [a,b,c,*], Pin Zhao [a,b], Bila Ga [a,b], Junmei Jia [d], John P. Giesy [e,f,g,h]

[a] *Laboratory of Solid Waste Treatment and Recycling, Research Center for Eco-Environmental Sciences, Chinese Academy of Sciences, Beijing 100085, China*
[b] *University of Chinese Academy of Sciences, Beijing 100049, China*
[c] *State Key Laboratory of Urban and Regional Ecology Research, Center for Eco-Environmental Sciences, Chinese Academy of Sciences, Beijing 100085, China*
[d] *State Key Laboratory of Plateau Ecology and Agriculture, Qinghai University, Xining 810016, China*
[e] *Toxicology Program Faculty, Toxicology Centre, University of Saskatchewan, Saskatoon, SK S7N 5B3, Canada*
[f] *Department of Veterinary Biomedical Sciences, University of Saskatchewan, Saskatoon, SK, Canada*
[g] *Department of Integrative Biology, Michigan State University, East Lansing, MI, USA*
[h] *Department of Environmental Science, Baylor University, Waco, TX, USA*

HIGHLIGHTS

- Microplastics in sediments from lakeshores to center of the lake was investigated.
- Microplastic trends in sediments of different areas of Qinghai Lake were different.
- Lake surface sediments were dominated by small transparent fibers of polypropylene.
- Microplastic distributions associated with hydrodynamics and environmental factors

GRAPHICAL ABSTRACT

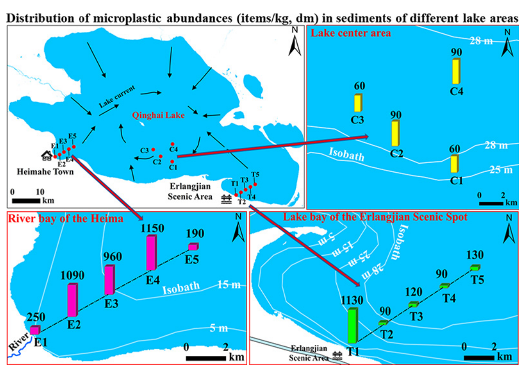

ARTICLE INFO

Editor: Yolanda Picó

Keywords:
Plastic debris
Remote Lake
Transport
Sedimentation
Hydrological processes
Environmental factors

ABSTRACT

Although several studies of microplastics (MPs) with size <5 mm in lake sediments focused on lakeshore areas, there have been no studies of distributions of MPs from lakeshores to the center of a lake. To test our hypothesis that MPs decrease from lakeshore to the center, a study was conducted on the largest brackish lake on the remote and high-altitude Tibetan Plateau, China. Abundances and characteristics of MPs in 14 samples of surface sediment collected from a river bay, a lake bay, and a lake central area were investigated. Distributions were influenced by river inflow, tourism, and minimal activity of humans, respectively around Qinghai Lake. The mean abundance of MPs in sediments of Qinghai Lake was 393 ± 457 items/kg, dry mass (dm). Based on the range of MP abundances in surface sediments of lakes worldwide, Qinghai Lake was classified as being moderately polluted with MPs. The dominant color, shape, size, and polymer type of MPs in sediments were transparent, fiber, 0.05–1 mm, and polypropylene, respectively. The river bay had a mean abundance of MPs two-fold greater than either the bay or central area of the lake. This indicates that the river catchment caused more pollution with MPs, while the central area of the lake was not a sink for MPs. Spatial trends of MPs in sediments from the shore to the center of the lake differed among areas, and were significantly related to wind, lake current, sedimentation rate, water- and sediment-properties, water depth, and proximity to land sources of MPs.

* Corresponding author at: Laboratory of Solid Waste Treatment and Recycling, Research Center for Eco-Environmental Sciences, Chinese Academy of Sciences, Beijing 100085, China.
E-mail address: luow@rcees.ac.cn (W. Luo).

http://dx.doi.org/10.1016/j.scitotenv.2022.155434
Received 29 January 2022; Received in revised form 17 April 2022; Accepted 18 April 2022
Available online 21 April 2022

1. Introduction

Microplastics (MPs) (< 5 mm) are ubiquitous in standing aquatic environments on a global scale. The threat of MPs to aquatic ecosystems and human health is under increasing scrutiny. As important standing water systems, lakes play a key role in water supply, aquaculture, hydrological cycle, and ecosystem services. Being semi-closed systems with varying hydrographic conditions and different patterns of circulation, lakes are regarded as sinks for MPs (Fischer et al., 2016). Abundances and morphological characteristics of MPs have been documented in lakes worldwide (Anderson et al., 2016; Fischer et al., 2016; Free et al., 2014; Mason et al., 2020; Mason et al., 2016; Vaughan et al., 2017), which were generally influenced by intensive human activities especially urbanization and population. In recent years, there is growing evidence that lakes of various dimensions in remote regions contain striking abundances of MPs (Faure et al., 2015; Fischer et al., 2016; Liang et al., 2021). However, contamination of remote lakes by MPs did not draw public attention, due to lesser populations and fewer sources of MPs around those lakes (Dusaucy et al., 2021).

More than 1500 lakes on the remote Tibetan Plateau (TP) account for about 49% of the total lake area of China and are important sources of drinking water at an average altitude of more than 4000 m, a.s.l (above sea level), and thus is called the "Asian Water Tower" (Song et al., 2014). They play crucial roles in water security, ecological services, and human health for many Asian countries. Qinghai Lake is the largest lake in China. Due to lack of proper sewage and solid waste treatment facilities around the lake (Wu et al., 2006), MPs from land sources including local residents and tourism activities have been transferred to Qinghai Lake through runoff, sewage discharge, discarded plastic products, and atmospheric deposition (Xiong et al., 2018). Consequently, MPs have been detected in surface water and lakeshore sediments of Qinghai Lake (Feng et al., 2020; Xiong et al., 2018). Sediments of lakes represent an archive that can be used to detect and quantify natural and anthropogenic changes at the scale of watersheds of lakes. Moreover, sediments are expected to be temporary and long-term sinks for MPs (Turner et al., 2019; Vaughan et al., 2017). Also, resuspension of sediments is a potential source of MP pollution in lake waters. It is estimated that approximately 70–90% of MP particles can eventually accumulate in sediments (Uddin et al., 2021), which are accessible to benthic suspension and deposit feeders (Van Cauwenberghe et al., 2015), and to other sediment-dwelling organisms (Wright et al., 2013). It has been reported that in a lake of significantly larger scale, abundances of MPs in sediments decreased with distance from the shore (Eerkes-Medrano et al., 2015; Free et al., 2014). While this distribution seems reasonable given the sources of MPs at these sites, further research is required to determine whether this distribution exists more broadly in lake systems. Investigating abundances of MPs and spatial resolution within a lake means focusing on a smaller scale, favoring investigation of total budgets and taking into account regional or local factors influencing pathways of input (Fischer et al., 2016). Furthermore, factors controlling distributions of MPs in lakes are likely to vary among areas of the lake (Bertoldi et al., 2021; Hengstmann et al., 2021; Imhof et al., 2017). However, relatively little is known about accumulation and transport mechanisms and influencing factors of MPs in surface sediments within various areas of a lake on the TP. This information is crucial for future modeling of movement of MPs, assessing risks, and estimating influences and efficacies of implemented conservation methods for a remote alpine lake ecosystem (Free et al., 2014; Galafassi et al., 2021; Imhof et al., 2013).

In this study, distribution of abundances of MPs in surface sediments of Qinghai Lake, which is representative of lakes influenced by river discharges and tourism activities on the TP, was investigated. Several hypotheses were tested: 1) MPs might be accumulated in lake sediments and decrease with increasing distance from lakeshores to the center of the lake; 2) there are different magnitudes of pollution and morphological characteristics of MPs in sediments among areas of the lake; and 3) geographic locations (sampling points), hydrodynamic conditions including water depth and current, and environmental factors including wind, water- and sediment- properties might affect distribution of MPs in sediments of different areas of the lake. Findings in this study could improve understanding of pathways and fates of MPs in a remote, high-altitude lake like the Qinghai on the TP, China and take effective measures to control and manage MPs.

2. Materials and methods

2.1. Study area

Qinghai Lake (36°32′ ~ 37°35′N, 99°36′ ~ 100°47′E) is situated in an endorheic basin of Qinghai Province, China, a sensitive semi-arid zone with average altitude of approximately 3200 m. The lake, which has an area of approximately 4500 km^2 with an average water depth of 21 m, is classified as an alkaline, salt lake (Jian et al., 2021; Sha et al., 2017). Local weather is influenced by the Asia summer monsoon and Westerlies winds. Average ambient temperatures in the basin range from −5 to 8 °C. Annual rainfall varies from 250 to 550 mm (Jian et al., 2021). The density of human habitation around the lake is about 9.3 inhabitants per km^2. There are neither cities nor industries around the lake, and animal husbandry and tourism are major activities (Xiong et al., 2018). The lake is a hydrologically closed drainage system, and there is no outflow. More than 40 rivers flow mainly from the north and northwest into the lake. Most rivers are ephemeral with the exception of the Heima River which is one of the permanent streams passing through the town of Heimahe, in which tourism is a pillar industry (Li et al., 2009). Although the resident population of the town of Heimahe decreased from 5163 to 4704 during the period of 2010–2020 (Bureau of Statistics of Qinghai Province, 2020), the number of visitors to the town increased in recent years. For example, an average of 1780 tourists visited the town every day during the tourism season in 2018 (Wu, 2018). The distance from downtown Heimahe to Qinghai Lake is approximately 1 km. The Erlangjian scenic area is the largest tourism area around the lake and the most important destination for tourists. The center of the lake is located around Haixinshan Island, where there is minimal human activity (Fig. 1).

2.2. Sample collection

Based on land use, human activities, and environmental factors within the catchment of Qinghai Lake, 14 sampling sites were selected from river bay of Heima (RB-HM), lake bay at the Erlangjian Scenic Spot (LB-ESS), and central area of the lake (CAL), representing effects of inputs from the Heima River catchment, tourism activities from the ESS, minimal human activity in the center of the lake on the distribution of MPs in various areas of the lake, respectively (Fig. 1). Furthermore, the RB-HM, LB-ESS, and CAL are characterized by different hydrodynamic and sedimentation conditions. The Heima River has an average annual flow rate of 0.34 m^3/s, and its inlet flow is 1.5×10^7 m^3, accounting for 0.7% of total inlet flow of all rivers into the lake (Li et al., 2006). The LB-ESS, located in southeast of Qinghai Lake, is strongly influenced by wind and water currents. The CAL is a sedimentation area with the lowest water velocity (Han et al., 2016; Han et al., 2015; Lanzhou Institute of Geology et al., 1979).

Five surface sediment samples (E1–E5) were collected at five sites along one straight line from the Heima River Estuary to the open lake in the RB-HM, and another five samples (T1–T5) were collected at another five sites along another straight line from lakeshore of the Erlangjian Scenic Spot to the open lake within the LB-ESS. The interval between two consecutive sampling sites is about 2 km. Because of relatively homogenous sediments influenced by minimal human activity and the lowest water velocity (Han et al., 2016; Han et al., 2015; Lanzhou Institute of Geology et al., 1979), four surface sediment samples (C1–C4) were randomly collected from the CAL (Fig. 2).

Sampling was conducted in September 2020 (Fig. 1 and Table 1), with a detailed description of sampling methods given in Text S3.

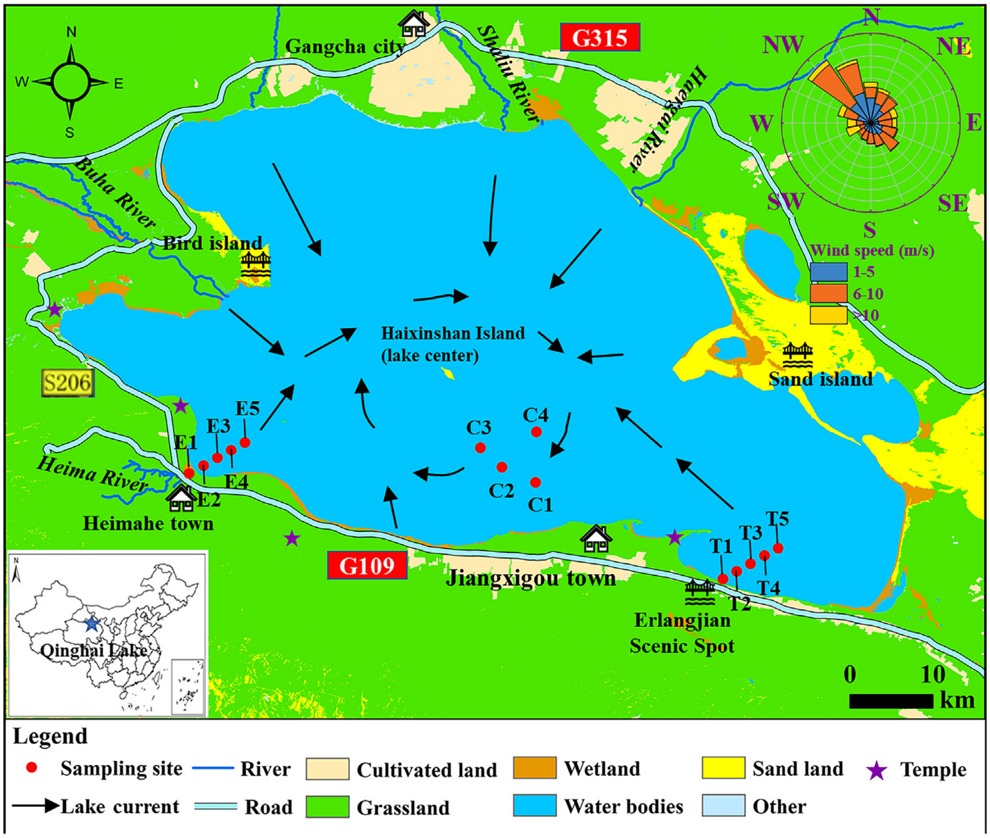

Fig. 1. Sediment sampling sites, lake currents, wind rose diagram, and land use within Qinghai Lake watershed, China.

2.3. Water environmental factors

Because we hypothesized that these environmental factors could influence or better explain the distribution of MPs in sediments, depth of water, conductivity, salinity, and turbidity, textures of sediments, and distance to source of MPs were measured (Chen et al., 2021; Gerolin et al., 2020; Kanhai et al., 2018; Quesadas-Rojas et al., 2021; Sarkar et al., 2019). Depths of water from top of water to lake bottom were measured at each location, by use of a portable depth sounder (SM-5A, Speedtech, USA). Distances from the lakeshore to each sampling site were measured from satellite images from Google Earth. Surface water (0–5 cm) parameters including salinity, conductivity, and turbidity at each site were measured using a calibrated portable multiprobe analyzer (HQ40d, Hach, USA) and a portable turbidimeter (WZB175, Leici, China). Using a Mastersizer 2000 laser diffraction system (Malvern Instruments, Malvern, UK), grain size distribution of each sediment sample was determined according to a modified procedure proposed by Sun et al. (2020).

2.4. Extraction of microplastics

Before extraction, sediment was dried for 72 h, to a constant mass in an oven at 50 °C (Yang et al., 2021a). Then, the dried samples were subjected to analysis according to a modified procedure proposed by the NOAA (Masura et al., 2015). Briefly, two duplicate aliquots of 50 g of each dried and thoroughly mixed sample of sediment were transferred to two 800-mL glass flasks, mixed with 300 mL of $ZnCl_2$ solution (density 1.6 g cm^{-3}) in each flask, and left overnight for sedimentation (Chubarenko et al., 2016; Yang et al., 2021b). The supernatant in each flask was filtered through a stainless-steel sieve with a mesh size of 50 μm. Residual solids on the sieve were transferred to a clean beaker. 20 mL of a 0.05 M Fe (II) solution in acidic medium (0.1 M H_2SO_4) and 20 mL of 30% H_2O_2 were added, until all the organic substances were digested. The digested sample was vacuum filtered through a nylon filter (20 μm pore size), which was washed with $ZnCl_2$ solution. The resulting eluent settled for 24 h in a separatory funnel. The remaining sample was filtered through a cellulose acetate filter (0.45 μm pore size), which was then dried at room temperature in a clean Petri dish with a cover until constant mass, then kept in a desiccator for further identification and observation. A detailed description of the sample processing is given in Text S1.

2.5. Observation and identification of microplastics

All MPs on the filter were observed under an optical stereo-microscope (SZX7, OLYMPUS, Japan), and measured. Individual photographs were then taken using a digital microscope (DP26, OLYMPUS, Japan). Based on results of previous studies (Wang et al., 2020), MPs are divided into four categories of shape: pellets, fragments, films, and fibers, eight categories of color: transparent, blue, red, green, black, yellow, white, and the others, and seven categories of size: 0.05–0.1 mm, 0.1–0.2 mm, 0.2–0.3 mm, 0.3–0.5 mm, 0.5–1 mm, 1–2 mm, and 2–5 mm (Hidalgo-Ruz et al., 2012).

To determine polymer types of sorted MP particles identified by stereo-microscope, an attenuated total reflection micro-Fourier transform infrared (ATR-μ-FTIR) spectrometer (Nicolet IN10 MX, Thermo Scientific, USA) was used to obtain spectral characteristics of a fraction of the sorted MP particles. IR-Spectra were recorded over the wavelength range of 4000–675 cm^{-1} at a resolution of 4 cm^{-1}, applying 64 scans. Obtained spectra were compared with libraries of spectra, including Sprouse Polymers by ATR, Common Materials, and Hummel Polymer and Additives, which were provided by the manufacturer. For accurate identification of the polymer, the match factor threshold was calculated as 0.70.

2.6. Quality assurance and control

During the processes of sampling and treatment, to avoid potential background contamination and self-contamination by clothes and plastics,

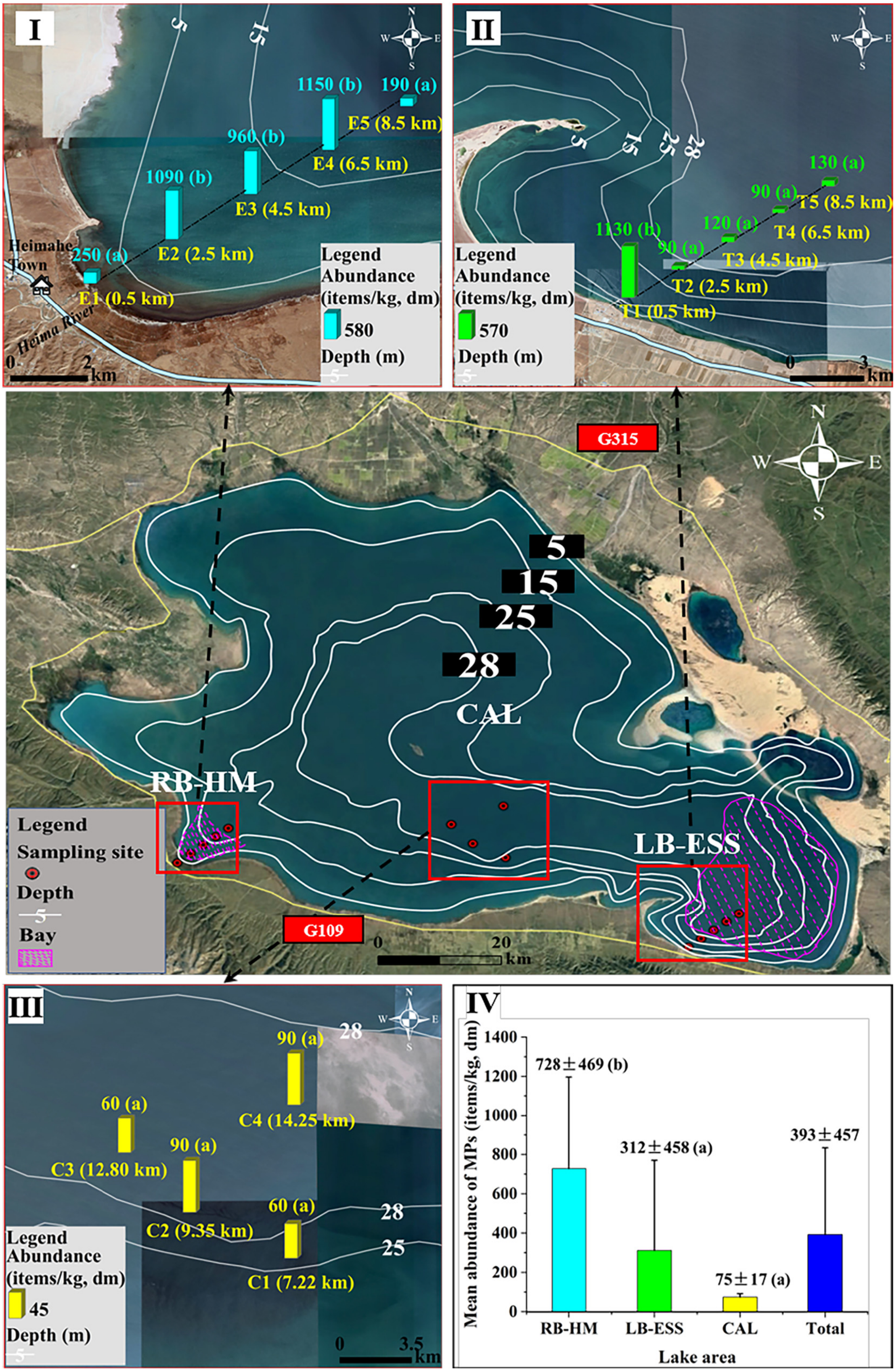

Fig. 2. Distributions of microplastic abundances in sediment samples collected from river bay of the Heima (RB-HM) (I), lake bay at the Erlangjian Scenic Spot (LB-ESS) (II), center area of the lake (CAL) (III) and mean ± SD abundances of microplastics in sediment samples from different areas of Qinghai Lake (IV) (Same letter in parentheses indicates no significant difference (ANOVA, $p > 0.05$)).

and analyses of samples (Scopetani et al., 2020), the following preventive measures were taken: 1) the use of plastic products during sampling was prohibited and all sampling tools and containers were washed using ultrapure water; 2) all sample extractions were performed under a laminar flow hood in a clean room in order to avoid contamination; 3) all solutions used in this study were filtered through a 0.45 μm filter; 4) cotton lab coats

Table 1
Sediment sampling information and water environmental factors in Qinghai Lake.

Sediment sampling information			Surface water parameter			Surface sediment parameter		
Sampling site	Depth (m)	Distance to lakeshore (km)	Conductivity (ms/cm)	Salinity (‰)	Turbidity (NTU)	Clay (<2 μm) (%)	Silt (2–20 μm) (%)	Sand (20–2000 μm) (%)
E1	0.30	0.50	1.58	0.89	24.00	3.09	18.67	78.24
E2	7.75	2.50	13.45	9.58	2.90	5.26	35.68	59.05
E3	12.85	4.50	13.96	9.98	2.46	7.73	47.09	45.18
E4	18.15	6.50	13.98	10.00	1.25	8.76	53.97	37.27
E5	18.24	8.50	14.00	10.00	1.45	6.99	44.54	48.47
RB-HM	11.5 ± 7.6	4.5 ± 3.2	11.4 ± 5.5	8.1 ± 4.0	6.1 ± 9.9	6.4 ± 2.2	40.0 ± 13.6	53.6 ± 15
T1	15.90	0.50	14.06	9.91	1.94	7.35	44.09	48.56
T2	27.10	2.50	13.96	9.93	1.82	16.36	58.97	24.67
T3	28.10	4.50	14.02	10.03	1.62	11.81	60.37	27.82
T4	28.40	6.50	14.11	9.97	1.65	15.89	57.04	27.06
T5	28.40	8.50	14.06	10.12	1.29	15.78	57.25	26.97
LB-ESS	25.6 ± 5.4	4.5 ± 3.2	14.0 ± 0.06	10.0 ± 0.09	1.7 ± 0.3	13.4 ± 3.9	55.5 ± 6.6	31.0 ± 10
C1	26.80	7.22	14.27	10.04	1.17	17.20	57.09	25.71
C2	28.10	9.35	14.30	10.06	1.04	16.19	56.55	27.25
C3	28.00	12.80	15.61	10.13	1.08	12.31	56.06	31.63
C4	28.00	14.25	15.53	10.12	1.09	15.53	65.44	19.03
CAL	27.7 ± 0.6	10.9 ± 3.2	15.0 ± 0.63	10.1 ± 0.04	1.1 ± 0.05	15.3 ± 2.1	58.8 ± 4.5	25.1 ± 5.2
Total	21.2 ± 9.2	5.4 ± 4.3	13.3 ± 3.4	9.3 ± 2.4	3.2 ± 6.0	11.5 ± 4.8	50.9 ± 12	37.6 ± 16

Note: RB-HM: river bay of the Heima; LB-ESS: lake bay of the Erlangjian Scenic Spot; CAL: center area of the lake.

and rubber gloves were worn during the processes of sampling, treatment and analysis of samples; 5) when not in use, all containers used in the present study were sealed with or in aluminum foil; 6) field and laboratory blanks were conducted according to the detailed procedures shown in Text S2; and 7) recovery tests were also ascertained by spiking PP fragment and PET fibers with similar dimension (0.1–0.5 mm) into the environmental samples. Average recoveries of PP fragment and PET fibers were 91.1% and 93.3%, respectively.

2.7. Data analysis

Abundances of MPs were expressed as numbers of MP particles per kilogram of dry mass of sediment (items/kg, dm). Ln-transformed data for abundances of MPs were tested for normality using Shapiro-Wilk normality test and for homogeneity of variance with the Levene test and ln-transformed data met criteria for subsequent applications of parametric statistics. An analysis of variances (ANOVA-one way) and Fisher's Least Significant Difference (LSD) test was performed to evaluate statistical differences in abundance of MPs between sampling sites and lake areas ($p < 0.05$). Since data for environmental factors were not normally distributed, non-parametric statistics were applied. Spearman's rank correlation analyses were used to investigate relationships between independent variables (water depth, distance to lakeshore, conductivity, salinity, turbidity, and sediment grain size) and dependent variables (abundances of MPs). A Kruskal-Wallis test was used to test for differences of water environmental factors among areas. All statistical analyses were performed using SPSS 25. Graphs were drawn using Origin Pro 2020. ArcGIS 10.6 was applied according to longitude and latitude collected by GPS to draw sampling and spatial distribution maps of MP abundances within the lake. The vector data for the lake catchment and land use (Fig. 1) was downloaded from the National Tibetan Plateau Data Center (TPDC) (Liu et al., 2014).

3. Results

3.1. Abundances of microplastics in surface sediments

MPs were detected in all sediments collected from Qinghai Lake. The mean abundance of MPs in the samples was 393 ± 457 items/kg, dm (mean ± standard deviation), with a range of 60 ± 28–1150 ± 127 items/kg, dm (Fig. 2). Greatest abundances of MPs in sediments of Qinghai Lake were observed at sites E4 (1150 ± 127 items/kg, dm) and T1(1130 ± 127 items/kg, dm), whereas the lowest were at sites C1 and C3 (60 items/kg, dm) (Fig. 2). Mean abundances of MPs in sediments of the RB-HM, LB-ESS, and CAL were 728 ± 469, 312 ± 458, and 75 ± 17 items/kg, dm, respectively. The mean abundances of the LB-ESS and CAL were not significantly different (ANOVA, $p > 0.05$). The mean abundance in the RB-HM was more than two-fold greater than in the LB-ESS and CAL (ANOVA, $p < 0.05$) (Fig. 2IV). In the RB-HM, the abundance of MPs in sediment abruptly increased from lakeshore site E1 (0.5 km away from the Heima River Estuary) (250 ± 71 items/kg, dm) to site E2 (2.5 km away from the estuary) (1090 ± 127 items/kg, dm), peaked and kept steady at sites E2–E4 (2.5–6.5 km from the estuary) (960 ± 226–1150 ± 127 items/kg, dm), and then sharply decreased at site E5 (8.5 km away from the estuary) (190 ± 42 items/kg, dm) (Fig. 2I). Abundances at sites E2–E4 were not significantly different (ANOVA, $p > 0.05$). Abundances at sites E2–E4 were not just three-fold greater, but were also significantly greater than at sites E1 and E5 (ANOVA, $p < 0.01$). In the LB-ESS, the abundance steeply decreased from site T1 (0.5 km away from the lakeshore of the ESS) (1130 ± 127 items/kg, dm) to site T2 (2.5 km away from the lakeshore) (90 ± 14 items/kg, dm), and then varied from 90 ± 14 to 130 ± 28 items/kg, dm at sites T2–T5 (2.5–6.5 km away from the lakeshore). Abundances at sites T2–T5 were not significantly different (ANOVA, $p > 0.05$). Abundance at site T1 was not just eight-fold greater, but also significantly greater than at sites T2–T5 (ANOVA, $p < 0.05$) (Fig. 2II). It seems that the trend of MP abundances from lakeshore to the center in the RB-HM is contrary to that in the LB-ESS. In the CAL, although abundances in sediments ranged from 60 ± 28 to 90 ± 71 items/kg, dm at sites C1–C4, they were not significantly different (ANOVA, $p > 0.05$) (Fig. 2III).

3.2. Characteristics of microplastics in surface sediments

Among shape categories of MPs in sediments of Qinghai Lake, fibers were dominant with a mean proportion of 83%, followed by fragments with a mean proportion of 17% (Fig. 3A and B). Fragments were observed at all sites, except for sites T4 and C4 (Fig. 3A). Films and pellets were found exclusively at sites E3 and T3 with mean proportions of 0.2% and 0.4%, respectively (Fig. 3A). Mean proportions of fibers in the RB-HM, LB-HM, and CAL were 85%, 78%, and 80%, respectively (Fig. 3B). There were no significant differences in mean proportions of fibers between areas of the lake (ANOVA, $p > 0.05$).

Transparent (52%) was the dominant color of MPs across all the sediment samples, follow by blue (22%), green (9%), black (5%), red (5%), yellow (2%), white (1%), and others (4%) (Fig. 3D). Blue was prevalent at sites T5, C2, C3, and C4, while green was dominant at site E1 (Fig. 3C). Mean proportions of transparent MPs in the RB-HM, LB-ESS, and CAL were 55%, 49%, and 40%, respectively, which were not significantly different (ANOVA, $p > 0.05$). Mean proportions of blue MPs in the RB-HM, LB-ESS, and CAL were 20%, 21%, and 50%, respectively (Fig. 3D), with the

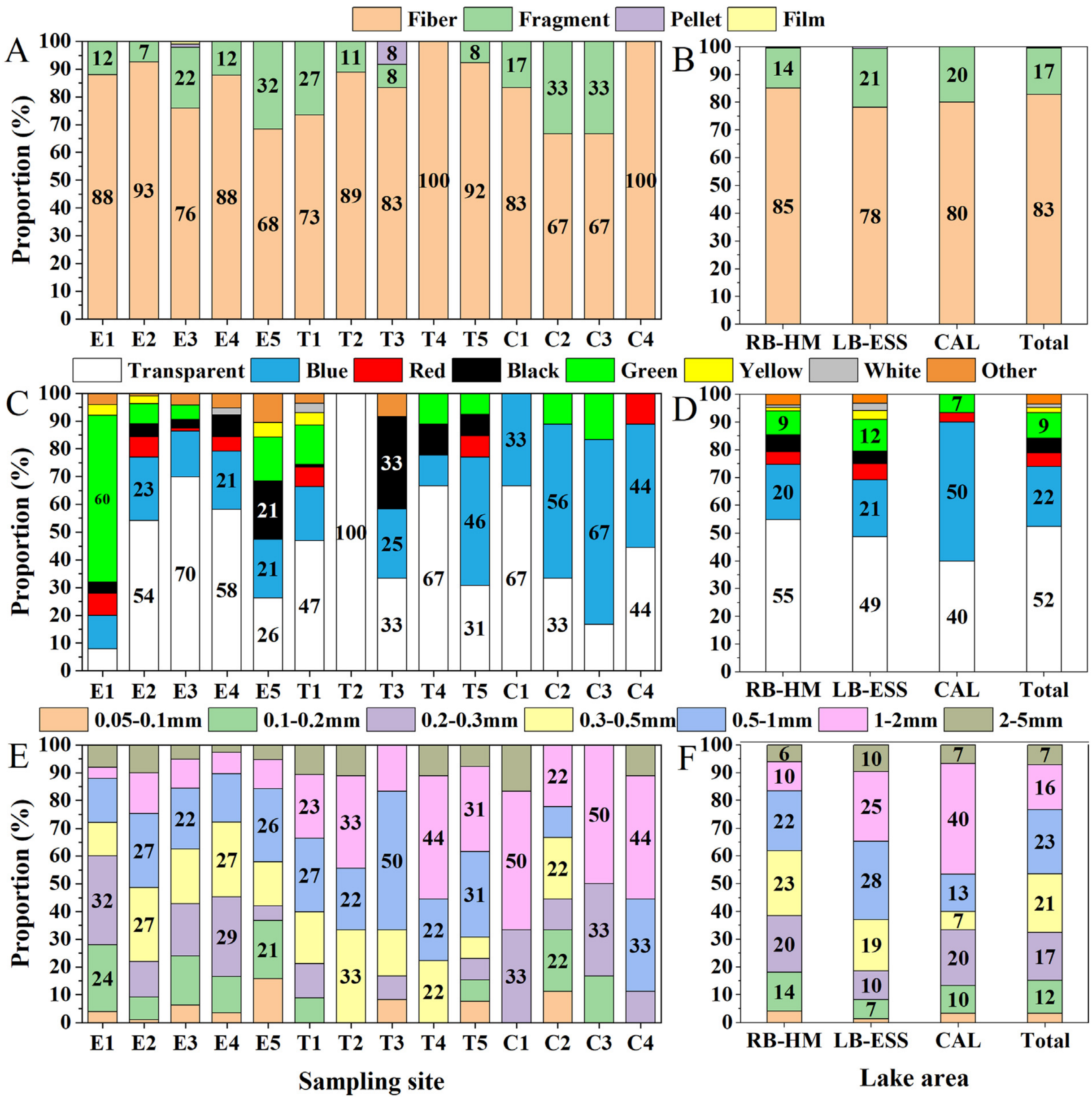

Fig. 3. Proportions of microplastic shape, color, size, and polymer type in sediment samples from different sites (A, C, E) and lake areas (B, D, F) of Qinghai Lake (RB-HM: river bay of the Heima; LB-ESS: lake bay at the Erlangjian Scenic Spot; CAL: center area of the lake).

proportion significantly greater in the CAL than in the RB-HM and LB-ESS (ANOVA, $p < 0.05$).

The size range of 0.5–1 mm (23%) of MPs in all the samples of sediment had the greatest proportion, followed by the size ranges of 0.3–0.5 mm (21%), 0.2–0.3 mm (17%), 1–2 mm (16%), 0.1–0.2 mm (12%), 2–5 mm (7%), and 0.05–0.1 mm (4%), respectively (Fig. 3F). Small MPs (0.05–1 mm in size) were most frequently observed, with a proportion of 77%. The CAL had the greatest proportion of large MPs (1–5 mm in size) in its sediments (47%), followed by the LB-ESS and RB-HM (Fig. 3F).

Previously proposed statistical analysis (Gardon et al., 2021; Kedzierski et al., 2019) was used to determine the number of MP particles that must be analyzed by ATR-μ-FTIR in our study and found that the number was 41. To improve accuracy of identification of polymer type, we still randomly selected 105 (two folds greater than 41) suspended MP particles, except for some of those that were too small to move (<100 μm), from total suspended MP particles which were thoroughly mixed before selection (Yang et al., 2021a). The suspended 105 MP particles accounted for 19.1% of total suspected MP particles and represented more common colors, sizes, and shapes of MPs in all sediment samples. Ninety percent of the 105 suspected particles were confirmed as MPs, and the remaining particles were identified as cotton, quartz, and calcium carbonate. A total of 10 polymer types were identified in the confirmed MP particles, among which polypropylene (PP, 27%) was the prevalent, followed by polyamide (PA, 24%), polyethylene terephthalate (PET, 24%), polyethylene (PE, 17%), and the other polymers (7%) including polystyrene (PS), polyvinyl chloride (PVC), polyvinyl acetate (PVAc), poly(1,1-difluoroethylene) (PVDF), alkyd varnish, and cellophane (Fig. 4I). The FTIR-spectra of some typical MP polymer types are shown in Fig. 4II and 4III. Eight types of polymers, PA, PP, PE, PET, PS, PVDF, PVAc and Cellophane, were observed in sediments of the LB-HM, among which PA and PP were the dominant polymer types (Fig. 4I). Six types of polymers, PA, PP, PE, PET, alkyd varnish and PVC, were observed in sediments of the LB-ESS, while only four types, PA, PP, PE and PET were found in the CAL. PET and PE were the prevalent polymer types of MPs in the sediments of the LB-ESS and CAL (Fig. 4I).

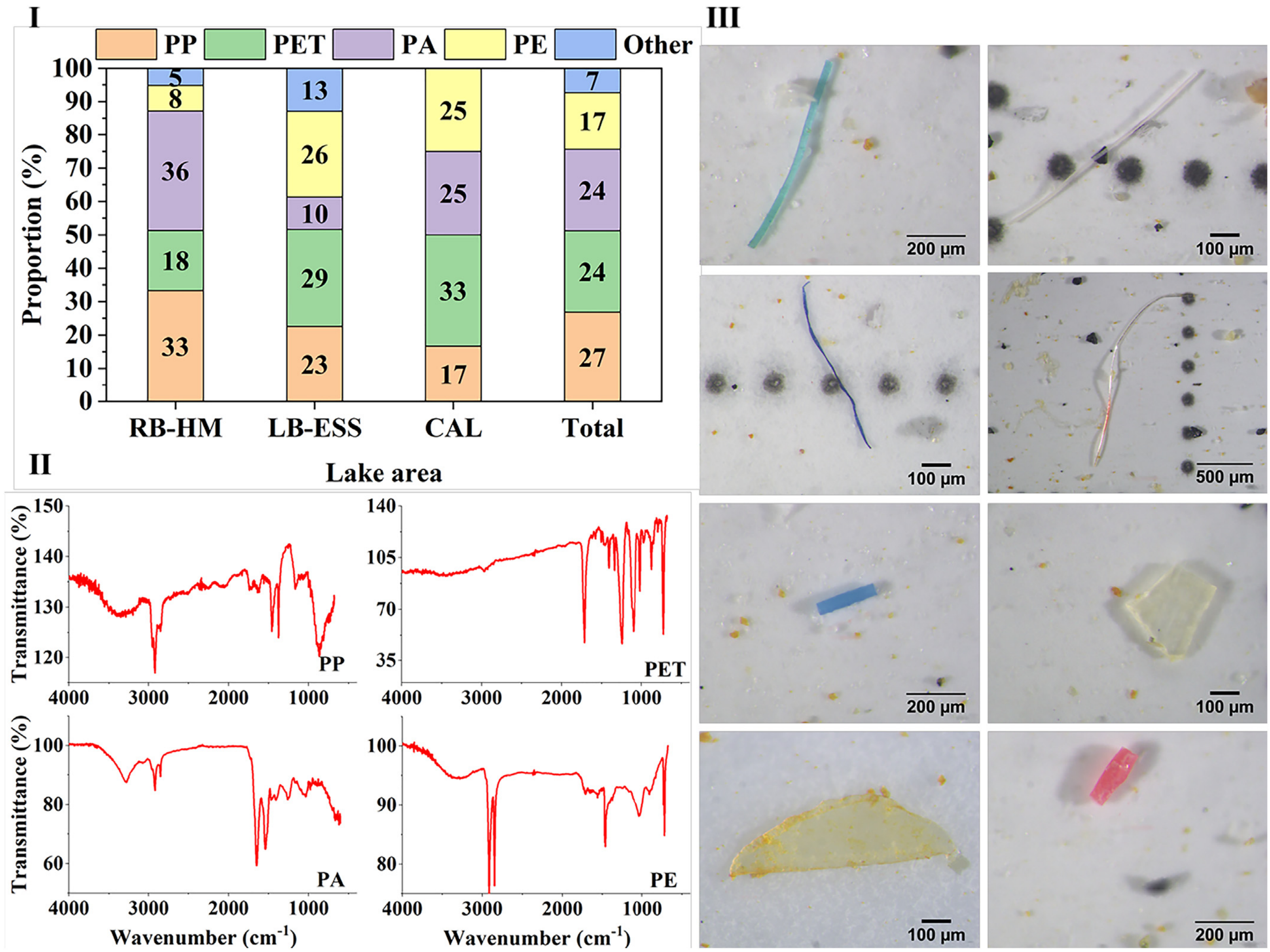

Fig. 4. Proportions of polymer types of MPs in sediment samples from different lake areas (I), infrared spectrum of PP, PET, PA, and PE (II), and images of typical MPs (II) found in sediment samples of Qinghai Lake.

3.3. Relationships to water environmental factors

Mean depth of water at all sampling sites was 21.2 ± 9.2 m (Table 1). Mean values of conductivity, salinity, and turbidity for surface water of Qinghai Lake were 13.3 ± 3.4 ms/cm, 9.3 ± 2.4‰, and 3.2 ± 6.0 NTU, respectively (Table 1). Water depths, salinities, and conductivities at sites of the LB-EES and CAL were significantly greater than at sites of the RB-HM ($p < 0.05$). Turbidities at sites of the RB-HM were greater than at sites of the LB-EES and CAL. Based on classifications of soil textures (sand %, slit% and clay%) suggested by the International Union of Soil Sciences (Wu and Zhao, 2019), mean contents of clay (<2 μm), silt (2–20 μm), and sand (20–2000 μm) in the sediments were 11.5 ± 4.8%, 50.9 ± 12%, and 37.6 ± 16%, respectively (Table 1). Contents of clay and silt at sites of the LB-ESS and CAL were significantly greater than those at sites of RB-HM ($p < 0.05$), while contents of sand at sites of the LB-HM were remarkably greater than at sites of the RB-EES and CAL ($p < 0.05$).

Abundances of MPs in sediments of Qinghai Lake were significantly and negatively correlated with distance from sampling site to a lakeshore ($p < 0.01$), water depth ($p < 0.05$), salinity ($p < 0.05$) and conductivity ($p < 0.01$), but significantly and positively correlated with turbidity of water ($p < 0.05$) (Table S2). Abundances of MPs were significantly and negatively correlated with content of clay ($p < 0.01$) or silt ($p < 0.05$), but remarkably and positively correlated with content of sand in sediments of Qinghai Lake ($p < 0.01$) (Table S2).

4. Discussion

4.1. Distribution of microplastics in sediments of Qinghai Lake

Due to lack of standardization of methods, including density separation, collection, size fractions retained/reported, *etc.* and reporting across the studies of MPs, direct comparisons between the studies remain difficult (Hidalgo-Ruz et al., 2012). Globally, among 24 selected studies, which not only reported MPs in lake surface sediment (not including sediment core), but also used MP abundance unit similar to the current study, only 13 (54% of the total documents) reported means or ranges of MP abundance greater than that observed during the present study (Table S1). Nevertheless, mean abundance in the present study was greater than that in other remote lakes in the world, such as the black sea (Cincinelli et al., 2021), Lakes Mead and Mohave in USA (Baldwin et al., 2020) and the Lake Chiusi in Italy (Fischer et al., 2016), but similar to that in some urban lakes such as Lakes Wuliangsuhai (Mao et al., 2021) and Dongting in China (Hu et al., 2020; Jiang et al., 2018; Yin et al., 2020), Lake Vesijärvi in Finland (Scopetani et al., 2019), and Lake Simcoe in Canada (Felismino et al., 2021) (Table S1). Larger water body size, deeper water depth, and a dispersed pathway, and local wind effects resulted in lesser abundances of MPs in the black sea and the lakes in USA and Italy (Baldwin et al., 2020; Cincinelli et al., 2021; Fischer et al., 2016). In terms of global lake pollution of MPs, that in sediments of Qinghai Lake was classified as moderate (Xiong et al., 2018).

The non-linear trend of MP abundances from lakeshore to open lake in the RB-HM (Fig. 2I) may attribute to the hydrological processes of Qinghai Lake. Relatively low abundance of MPs at the site E1 might ascribe to high-energy hydrodynamic conditions, such as turbulence, waves, tides, storms, unstable and high velocity hydraulics in shallow waters (Enders et al., 2019; Harris, 2020; Martin et al., 2017), which might disturb benthic sediments, re-suspend, and relocate small MPs from the sediments, and thus reduce small MPs in the sediment at the Heima River Estuary (Eerkes-Medrano et al., 2015; Harris, 2020; Ho and Not, 2019). The great abundances of MPs at sites E2–E4 (Fig. 2I) in the LB-HM can be explained by the fact topographical features such as rough lakebeds, steep banks, complex shorelines and isobaths (He et al., 2021; Vermeiren et al., 2016; Yuan et al., 2019) within the semi-enclosed bay where the Heima river entered (Fig. 1 and Fig. 2) reduced strengths of wind, wave and water current, and thus increased residence time of MPs within the bay, resulting in accumulation of MPs in the sediments (Ballent et al., 2016; Lanzhou Institute of Geology et al., 1979). In addition, the great abundances at sites E2–E4 might also be related to their proximities to land sources of MPs around the RB-HM (Fig. 1) (Wong et al., 2020; Yonkos et al., 2014). However, the sharply decreased abundance at site E5 was due to that site E5 was more than 8 km away from the estuary and almost out of the bay, where the site was influenced by complex hydrodynamics caused by large input of the unpolluted Buha River, the largest river in the Qinghai Lake Basin. The Buha River had greater annual runoff of 1.12 billion m^3, accounting for 60% of total runoff of the whole lake, than the Heima River. The hydrological, meteorological, and topographical characteristics within the Buha River Basin led to the formation of water circulation in Qinghai Lake and the strong northwest wind (Average wind speed was 3.1–4.3 m/s with a range of 0–22 m/s) (Fig. 1) (Hengstmann et al., 2021; Lanzhou Institute of Geology et al., 1979).

A significantly decreasing trend of MP abundances from lakeshore to open lake was also observed in other lake-wide studies (Eerkes-Medrano et al., 2015; Free et al., 2014). The highest abundance of MPs at site T1 near the Erlangjian Scenic Spot (ESS) (Fig. 2II) was caused by annual 4.4 million visitors who used local services, purchased goods, and introduced or left waste materials behind in the ESS (Feng et al., 2020; Statistics, 2020). Previous studies have also proven that tourism is the main source of MPs in remote lakes (Free et al., 2014; Xiong et al., 2018). On the other hand, a long-term dominant northwestern wind (Fig. 1) would result in a landward oriented transportation and probable sedimentation of MP particles on the sediments at the lakeshore near the ESS (Bullard et al., 2021; Fischer et al., 2016; Rezaei et al., 2019). The low abundances of MPs in the sediments at sites T2–T5 in the LB-ESS may be explained by two factors (Eerkes-Medrano et al., 2015; Free et al., 2014). First, dilution of MPs became obvious with sharp increase of water depths from sites T1 (15.9 m) to T2 (27.1 m) and resulted in a significant decrease in MPs in sediments from sites T1 to T2 (Fig. 2II). Secondly, lake currents flowing from east to the west (Xiong et al., 2018) could facilitate the expulsion of MPs outside the LB-ESS (Fig. 1).

Results of a previous study indicate that currents might bring the floating plastic debris from the nearshore areas to center of Qinghai Lake and increase abundances of MPs in the water of the CAL (Xiong et al., 2018). However, the lowest mean abundance of MPs in the CAL in the present study (Fig. 2III) implied that the sediments in lake center of the Qinghai might not be a sink of MPs. The only reasonable explanation is that the CAL is far from terrestrial sources and thus receives fewer MPs. However, whether or not lesser rates of sedimentation ($0.0118\ g{\cdot}cm^{-2}{\cdot}year^{-1}$) (Enders et al., 2019; Harris, 2020; Sha et al., 2017; Xu et al., 2010), greater salinity and conductivity and depth, lesser turbidity of water (Table 1) and good water quality (Qi et al., 2015) in the CAL might explain the least abundance of MPs in sediments of the CAL still needs to be further explored in the future.

The highest mean abundance of MPs in the RB-HM was due to inflow of the polluted Heima River which can transport sewage discharge (320 m^3/d) and rubbish dumping (5.9 t/d) from the town of Heimahe (Wu et al., 2006; Xiong et al., 2018), where more than 200 residential hotels, motels, and restaurants have been developed in recent years (Huang, 2018) and without establishment of any wastewater treatment plant (WWTP) and rubbish collection and treatment system (Wu et al., 2006). In contrast, two WWTPs with treatment capability of 3000 m^3/day, and rubbish collection and treatment system have been running for more than 10 years in the ESS. It was reported that WWTP effluents after treated by joint system anoxic-aerobic bio-contact oxidation process was not directly discharged into the lake, but reused in grass lands of the ESS (Bao, 2020). This means that only 3% of the total load of MPs (MPs removal efficiency is usually 97% for WWTPs) reached the grass lands of the EES (Burns and Boxall, 2018). After application to grass lands, it is difficult for MPs to be released into the lake by runoff under the arid condition of Qinghai Province, China. That is why the lower mean abundance of MPs in the LB-ESS but the greatest mean in the RB-HM was observed.

Daily generation of 5848 m^3 sewage and 103 t rubbish, and booming tourism around Qinghai Lake (Wu et al., 2006) might be sources of MPs observed in sediments. Driven by the East Asian summer monsoon, Indian summer monsoon, winter monsoon, and the westerly jet stream (Wang et al., 2010), airborne MPs from the neighboring regions including India, and Qinghai and Gansu provinces in China could transport MPs over 1000 km to the TP (Dong et al., 2021; Wang et al., 2010), and thus increase MPs in Qinghai Lake. Notably, ubiquitous *lungtas* and prayer flags used for religious blessings in several temples located to the south of the lake (Fig. 1) and traditional yak tents for traveling and staying might be sources of MPs in sediments after their long-time exposure to extreme weather conditions on the TP (Jiang et al., 2019). All these sources of MPs mentioned above might explain why amounts of MPs in sediments of Qinghai Lake were moderate, compared to global levels of MPs in lake sediments.

4.2. Physical and chemical characteristics of microplastics in sediments of Qinghai Lake

The most common physical and chemical characteristics of fibers in the sediments (Fig. 3 and Fig. 4) included transparent and blue in color, 0.05–1 mm in size, and PP, PA, PET and PE in polymer types. These common characteristics of fibers in the sediments of Qinghai Lake were also reported in other lakes on the TP, indicating the same sources of fibers from washing clothes (Feng et al., 2021; Liang et al., 2021; Yang et al., 2021a), fishing in the past (Bissen and Chawchai, 2020; O'Bryan et al., 2010), atmospheric fallout (Dong et al., 2021; Wang et al., 2010), and locally discarded *lungtas* (wind horses or prayer flags) and tents (Jiang et al., 2019).

Homogeneous distributions of fibers in sediments of different areas of Qinghai Lake is due to larger ratios of surface to volume of fibers, which make them settle more slowly and be more prone to transport *via* air (Bullard et al., 2021) and water (Pohl et al., 2020). Furthermore, in addition to particle density, settling behavior of MPs is influenced by shapes and sizes (Khatmullina and Isachenko, 2017). Due to the elongated size, fibers in the suspension are more likely to be dragged downward to the sediment (Pohl et al., 2020). This mechanism results in an enrichment of MPs in sediment. The commonly observed fragments in the present study suggested that weathering and degradation of larger flexible plastic packaging could not be neglected (Dong et al., 2021; Zhang et al., 2021b). Pellets and films detected only at sites E3 and T3 might originate from personal-care products and agricultural mulches, which were sparsely used on the TP (Jiang et al., 2019; Lin et al., 2018).

It has been extensively reported that transparent was the dominant color of MPs in sediments on the TP (Feng et al., 2020; Feng et al., 2021; Jiang et al., 2019). That result implied that transparent MPs in sediments on the TP might have common sources such as packages, bags, ropes, bottles, coatings, adhesives, paints and composites (Bhutto and You, 2022; Zhang et al., 2018). Some colored MPs in sediments of the Qinghai Lake were more susceptible to be weathered, discolored and faded into transparent by extreme hypoxia, cold, heat and intense UV radiation on the TP (Min et al., 2020; Yang et al., 2015). The relatively great proportions of colored MPs such as the blue MPs composed of 81% fibers and 19% fragments and green MPs composed of 67% fibers and 33% fragments were found in lake sediments (Table S3). It means that sediments of the lake were influenced by modern life in which colored clothes (source of fibers) and colorful daily necessities, such as packages, bags, and bottles, which are sources of fragments after discarded, were used to increase the attractiveness and the longevity of plastic materials (Rodrigues et al., 2018; Zhang et al., 2018), especially those made for tourism.

The relatively small proportion of MPs in smallest size range of 0.05–0.1 mm in sediments is different from some previous studies, in which the MPs in the size range were found more abundant (Feng et al., 2021; Liang et al., 2021; Zhang et al., 2021b). This is likely attributed to rapid degradation of small plastic debris. On the TP, high ultraviolet radiation intensity and large diurnal variations in temperature might accelerate dissipation of small plastic debris (Zhang et al., 2016). Another reason is that identification of smaller MP particles by visual sorting is subjective and particles less than 0.1 mm cannot be discriminated visually from other sample material or are unmanageable with forceps due to their minuteness (Dris et al., 2018; Frei et al., 2019). Thus, these smallest MPs in sediments in the present study could be underestimated. The abundant small MPs (0.05–1 mm) (Fig. 3E and F) have also been observed during other studies of MPs in the lakes on the TP (Dong et al., 2021; Feng et al., 2020; Liang et al., 2021). The predominance of small MPs suggested that the degradation and fragmentation of their original plastic products might be accelerated under extreme weather conditions on the TP (Zhang et al., 2016). The greatest proportion of large MPs (1–5 mm) in the CAL (Fig. 3F) indicates that large MPs had greater ability to overcome turbulent mixing and were easily flushed to open lake with deep water (Bailey et al., 2021). Since abundances of MPs in the water column are related to depth of water column, represented and total water column depth (Lenaker et al., 2019), most of total number of larger MPs, which were fibers of PP and PE and had densities less than water in our study, might travel longer distances from high flow rate area at lakeshore to deep-water area with low flow rate in lake center and subsequently settled onto surface sediments (Han et al., 2016; Zhang, 2017).

PP, as the dominant polymer type in the present study (Fig. 4I), was also found in the rivers and lakes on the TP (Feng et al., 2021; Jiang et al., 2019). It is consistent with massive global production of PP products, such as ropes, bottle caps and netting (PlasticEurope, 2019). PP particles are easily colonized by microorganisms to form biofilms which increase both density and degradation of PP into small particles (Ivar do Sul and Costa, 2014). PA might be one of most important components of clothes and fishing gears, while PET might be a common material for single-use fabrics, packaging materials, and beverage bottles (Zhang et al., 2021a). Such dense plastics as PA (about 1.12–1.15 g cm^{-3}) and PET (1.38–1.41 g cm^{-3}) in water sink easily (Gao et al., 2021), leading to absolute dominance of MPs in sediment. The abundant PA and PP in the RB-HM might mainly originate from sewage effluents (Raju et al., 2020). PET and PE identified as dominant polymer types in the LB-ESS and CAL might come from discarded plastic bottles, food wrappers, and bags from tourism activities (Thushari et al., 2017). Greater diversity of polymer types in sediments of the RB-HM than that of the LB-ESS and CAL, indicates more sources of MPs from the river catchment.

4.3. Relationships to water environmental factors

Turbidity of water in Qinghai Lake was similar to those in other brackish lakes on the TP (Liu et al., 2021a). However, mean conductivities and salinities, observed during the present study, were greater than those in other studies of lakes on the TP (Liu et al., 2021a). Sediments of Qinghai Lake in the present study contained great contents of clay and silt, which are similar to those in brackish lakes such as the Selin Co (Wang et al., 2018) and the Pumayum Co on the TP (Ju et al., 2012).

In our study, a significant negative correlation between the abundance of MPs in sediment and the distance from a sampling site to lakeshore (Table S2) implied that MP distribution might depend on proximity to land sources of MPs (Wong et al., 2020; Yonkos et al., 2014). However, only one previous study reported that the variation of MPs concentration in riverine sediments can be related to water depth of the sampling sites (Gerolin et al., 2020). Shallow water areas are closer to terrestrial sources and are more likely to receive more MPs. In addition, MPs can become negatively buoyant upon fouling, and as water depth increases, MPs might be suspended in the lower and middle layers of the water column instead of settling onto surface sediment (Liu et al., 2021b). Furthermore, settlement of MPs from water onto surface sediment in a lake is a dynamic process which is influenced variously by aqueous environment, such as salinity (Andrady, 2011; Lenaker et al., 2019). Significant and negative correlations between MP abundance in sediment and water salinity and conductivity in the present study indicates that great salinity and conductivity in lake water increased buoyancy force of water, and thus fewer MPs were deposited onto surface sediment (Jiang et al., 2020). Meanwhile, high salinity can repress average growth rate of biofilm and decrease density, weight and sedimentation rate of MPs in water column (Li et al., 2019; Uurasjarvi et al., 2021). Significant positive correlation between the abundance of MPs in sediment and water turbidity in the present study was also reported by Pazos et al. (2018) who found that sedimentation of MPs tends to increase in the maximum turbidity front, which is linked to the greatest MP abundances in water (Bayo et al., 2020). Aggregation with particles could increase their sizes by forming hetero-aggregates and reducing solubility and inertness (Besseling et al., 2017; Horton et al., 2017), which results in greater sedimentation of MPs (Bayo et al., 2020).

A significant negative correlation between the abundance of MPs and the content of clay or silt in sediment in the present study is similar to that observed by Hengstmann et al. (2021); Quesadas-Rojas et al. (2021), but is contrary to that reported in other studies (He et al., 2020; Tibbetts et al., 2018; Vianello et al., 2013; Zobkov et al., 2020). Furthermore, a significant positive correlation between the abundance of MPs and content of sand in sediment in our study was also found in Bandon Bay and Rio Lagartos coastal lagoon (Chinfak et al., 2021; Quesadas-Rojas et al., 2021). As suggested by Quesadas-Rojas et al. (2021), the negative correlation is due to the positive correlation ($R = 0.71, p < 0.01$) between the distance from a sampling site to lakeshore and the content of clay in sediment (Table S2). Additionally, sand abrasion in the Qinghai Lake may break down large plastics into small particles during their transportation (Ding et al., 2019), and consequently increase the abundances in the sediments. To date, due to the limited number of published studies and the lack of comprehensive data sets on the interactions between the distribution and transport of MPs and other potential influential factors, such as flow velocity, wind and sediment clay, further in-depth investigations are needed to derive a detailed understanding of the deposition and transportation mechanics between different sediment particle types and MPs (He et al., 2020).

5. Conclusions

This work provides for the first time, data about distribution of MPs in surface sediments from lakeshore to the center of Qinghai Lake, the largest brackish lake on the TP, China, affected by river discharge, tourism and environmental factors. Mean abundance of MPs in the sediments was 393 ± 457 items/kg, dm, which was at a moderate MP pollution level compared to global lake sediment studies. The trend of MP abundances from lakeshore to the center in the river bay of Heima, was contrary to that in the lake bay at the Erlangjian tourism scenic spot, which was related to wind, lake current, sedimentation rate, water- and sediment-properties, water depth, and proximity to land sources of MPs. The different spatial trends of MPs in the sediments of different areas of the lake underline different transfer mechanisms of MPs from lakeshores to the center of the lake and the importance of investigating of MPs in different areas of the lake. The mean abundance in river bay of Heima (393 ± 457 items/kg, dm) was two-fold greater than that in lake bay at the Erlangjian tourism scenic spot (312 ± 458 items/kg, dm) and the central area of the lake (75 ± 17 items/kg, dm), emphasizing the need to improve management of sewage and rubbish within the river catchment. The least mean abundance was found in the lake center, indicating that the sediments in the center were not a sink of MPs. The most frequently observed colors, shapes, sizes, and polymer types were transparent, fiber, 0.05–1 mm, and polypropylene, respectively, which were related to sources of MPs, local people's traditions, customs and lifestyles, MP properties, atmospheric fallout, and degradation in extreme weather conditions on the TP. More polymer types of MPs in the sediments of river bay of Heima indicates more sources of MPs from the Heima River catchment. The abundance of MPs in the sediment of Qinghai Lake was associated with the distance to lakeshore, the depth, salinity, conductivity and turbidity of water, and the texture of sediment. The findings of this study could provide useful information for evaluating environmental risks posed by MPs and taking effective measures to control and manage contamination of MPs within a lake, which could also improve understanding of pathways and fates of MPs within a remote and high-altitude lake. Further studies should be more focused on behaviors of MPs within more different areas at a smaller scale of a lake and their impacts on benthic organisms and ecosystems.

CRediT authorship contribution statement

Ning Jiang: Methodology, Software, Formal analysis, Resources, Data curation, Writing – original draft, Visualization. **Wei Luo:** Conceptualization, Methodology, Software, Validation, Investigation, Writing – original draft, Writing – review & editing, Visualization, Supervision, Project administration, Funding acquisition. **Pin Zhao:** Investigation. **Ga Bila:** Investigation. **Junmei Jia:** Investigation. **John P. Giesy:** Writing – review & editing.

Declaration of competing interest

The authors declare that they have no known competing financial interests or personal relationships that could have appeared to influence the work reported in this paper.

Acknowledgements

This study was supported by Ministry of Science and Technology (2019QZKK0605), the National Key R&D Program of China (2017YFC0505803), National Natural Science Foundation of China (41761144078, 41705132 and 41675130, Project of Qinghai Science & Technology Department (2018-ZJ-958Q). Prof. Giesy was supported by the “High Level Foreign Experts” program (#GDT20143200016) funded by the State Administration of Foreign Experts Affairs, the P.R. China to Nanjing University and the Einstein Professor Program of the Chinese Academy of Sciences. He was also supported by the Canada Research Chair program and a Distinguished Visiting Professorship in the Department of Environmental Sciences at Baylor University, Waco, Texas, USA. We thank Prof. Aibin Zhan for allowing us to use stereomicroscope in his lab.

Appendix A. Supplementary data

Supplementary data to this article can be found online at https://doi.org/10.1016/j.scitotenv.2022.155434.

References

Anderson, J.C., Park, B.J., Palace, V.P., 2016. Microplastics in aquatic environments: implications for Canadian ecosystems. Environ. Pollut. 218, 269–280.
Andrady, A.L., 2011. Microplastics in the marine environment. Mar. Pollut. Bull. 62, 1596–1605.
Bailey, K., Sipps, K., Saba, G.K., Arbuckle-Keil, G., Chant, R.J., Fahrenfeld, N.L., 2021. Quantification and composition of microplastics in the Raritan Hudson Estuary: comparison to pathways of entry and implications for fate. Chemosphere 272.
Baldwin, A.K., Spanjer, A.R., Rosen, M.R., Thom, T., 2020. Microplastics in Lake Mead National Recreation Area, USA: occurrence and biological uptake. PLoS One 15, e0228896.
Bao, J.L., 2020. The Commencement Ceremony for the Project of Improvement of Sewage Treatment Efficiency and Water Quality in Erlangjian Wastewate Treatment Plant Was Held.
Bayo, J., Olmos, S., Lopez-Castellanos, J., 2020. Microplastics in an urban wastewater treatment plant: the influence of physicochemical parameters and environmental factors. Chemosphere 238, 124593.
Bertoldi, C., Lara, L.Z., Mizushima, F.A.L., Martins, F.C.G., Battisti, M.A., Hinrichs, R., Fernandes, A.N., 2021. First evidence of microplastic contamination in the freshwater of Lake Guaiba, Porto Alegre,Brazil. Sci. Total Environ. 759, 143503.
Besseling, E., Quik, J.T.K., Sun, M., Koelmans, A.A., 2017. Fate of nano- and microplastic in freshwater systems: a modeling study. Environ. Pollut. 220, 540–548.
Bhutto, S.U., You, X.Y., 2022. Spatial distribution of microplastics in Chinese freshwater ecosystem and impacts on food webs*. Environ. Pollut. 293.
Bissen, R., Chawchai, S., 2020. Microplastics on beaches along the eastern Gulf of Thailand - a preliminary study. Mar. Pollut. Bull. 157, 111345.
Bullard, J.E., Ockelford, A., O'Brien, P., McKenna Neuman, C., 2021. Preferential transport of microplastics by wind. Atmos. Environ. 245, 118038.
Bureau of Statistics of Qinghai Province, 2020. Qinghai Statistical Yearbook. China Statistic Publishing House, Xining.
Burns, E.E., Boxall, A.B.A., 2018. Microplastics in the aquatic environment: evidence for or against adverse impacts and major knowledge gaps. Environ. Toxicol. Chem. 37, 2776–2796.
Chen, H.L., Gibbins, C.N., Selvam, S.B., Ting, K.N., 2021. Spatio-temporal variation of microplastic along a rural to urban transition in a tropical river. Environ. Pollut. 289, 117895.
Chinfak, N., Sompongchaiyakul, P., Charoenpong, C., Shi, H., Yeemin, T., Zhang, J., 2021. Abundance, composition, and fate of microplastics in water, sediment, and shellfish in the Tapi-Phumduang River system and Bandon Bay,Thailand. Sci. Total Environ. 781, 146700.
Chubarenko, I., Bagaev, A., Zobkov, M., Esiukova, E., 2016. On some physical and dynamical properties of microplastic particles in marine environment. Mar. Pollut. Bull. 108, 105–112.
Cincinelli, A., Scopetani, C., Chelazzi, D., Martellini, T., Pogojeva, M., Slobodnik, J., 2021. Microplastics in the Black Sea sediments. Sci. Total Environ. 760, 143898.
Ding, L., Mao, R.F., Guo, X., Yang, X., Zhang, Q., Yang, C., 2019. Microplastics in surface waters and sediments of the Wei River, in the northwest of China. Sci. Total Environ. 667, 427–434.
Dong, H., Wang, L., Wang, X., Xu, L., Chen, M., Gong, P., Wang, C., 2021. Microplastics in a remote lake basin of the Tibetan Plateau: impacts of atmospheric transport and glacial melting. Environ. Sci. Technol. 55, 12951–12960.
Dris, R., Imhof, H.K., Löder, M.G.J., Gasperi, J., Laforsch, C., Tassin, B., 2018. Chapter 3 - microplastic contamination in freshwater systems: methodological challenges, occurrence and sources. In: Zeng, E.Y. (Ed.), Microplastic Contamination in Aquatic Environments. Elsevier, pp. 51–93.
Dusaucy, J., Gateuille, D., Perrette, Y., Naffrechoux, E., 2021. Microplastic pollution of worldwide lakes. Environ. Pollut. 284, 117075.
Eerkes-Medrano, D., Thompson, R.C., Aldridge, D.C., 2015. Microplastics in freshwater systems: a review of the emerging threats, identification of knowledge gaps and prioritisation of research needs. Water Res. 75, 63–82.
Enders, K., Kappler, A., Biniasch, O., Feldens, P., Stollberg, N., Lange, X., Fischer, D., Eichhorn, K.J., Pollehne, F., Oberbeckmann, S., Labrenz, M., 2019. Tracing microplastics in aquatic environments based on sediment analogies. Sci. Rep. 9, 15207.
Faure, F., Demars, C., Wieser, O., Kunz, M., De Alencastro, L.F., 2015. Plastic pollution in Swiss surface waters: nature and concentrations, interaction with pollutants. Environ. Chem. 12, 582–591.
Felismino, M.E.L., Helm, P.A., Rochman, C.M., 2021. Microplastic and other anthropogenic microparticles in water and sediments of Lake Simcoe. J. Great Lakes Res. 47, 180–189.
Feng, S., Lu, H., Tian, P., Xue, Y., Lu, J., Tang, M., Feng, W., 2020. Analysis of microplastics in a remote region of the Tibetan Plateau: implications for natural environmental response to human activities. Sci. Total Environ. 739, 140087.
Feng, S., Lu, H., Yao, T., Xue, Y., Yin, C., Tang, M., 2021. Spatial characteristics of microplastics in the high-altitude area on the Tibetan Plateau. J. Hazard. Mater. 417, 126034.
Fischer, E.K., Paglialonga, L., Czech, E., Tamminga, M., 2016. Microplastic pollution in lakes and lake shoreline sediments - a case study on Lake Bolsena and Lake Chiusi (central Italy). Environ. Pollut. 213, 648–657.
Free, C.M., Jensen, O.P., Mason, S.A., Eriksen, M., Williamson, N.J., Boldgiv, B., 2014. High-levels of microplastic pollution in a large, remote, mountain lake. Mar. Pollut. Bull. 85, 156–163.
Frei, S., Piehl, S., Gilfedder, B.S., Loder, M.G.J., Krutzke, J., Wilhelm, L., Laforsch, C., 2019. Occurence of microplastics in the hyporheic zone of rivers. Sci. Rep. 9, 11.
Galafassi, S., Sighicelli, M., Pusceddu, A., Bettinetti, R., Cau, A., Temperini, M.E., Gillibert, R., Ortolani, M., Pietrelli, L., Zaupa, S., Volta, P., 2021. Microplastic pollution in perch (Perca fluviatilis, Linnaeus 1758) from Italian south-alpine lakes. Environ. Pollut. 288, 117782.
Gao, J., Pan, S., Li, P., Wang, L., Hou, R., Wu, W.M., Luo, J., Hou, D., 2021. Vertical migration of microplastics in porous media: multiple controlling factors under wet-dry cycling. J. Hazard. Mater. 419, 126413.
Gardon, T., El Rakwe, M., Paul-Pont, I., Le Luyer, J., Thomas, L., Prado, E., Boukerma, K., Cassone, A.L., Quillien, V., Soyez, C., Costes, L., Crusot, M., Dreanno, C., Le Moullac, G., Huvet, A., 2021. Microplastics contamination in pearl-farming lagoons of French Polynesia. J. Hazard. Mater. 419, 126396.
Gerolin, C.R., Pupim, F.N., Sawakuchi, A.O., Grohmann, C.H., Labuto, G., Semensatto, D., 2020. Microplastics in sediments from Amazon rivers,Brazil. Sci. Total Environ. 749, 141604.
Han, Y.H., Li, X.Y., Wang, Q., Hao, L.W., Tian, B., 2015. Hydrodynamic control of sedimentary systems in shore zone of Qinghai Lake. Acta Sedimentol. Sin. 33, 97–104 (in Chinese).
Han, Y., Hao, L., Wang, Q., Ma, D., Ji, H., 2016. Prevailing winds controlled hydrodynamic characteristics of Qinghai Lake. Yellow River 38, 51–55 (In Chinese with English Abstract).
Harris, P.T., 2020. The fate of microplastic in marine sedimentary environments: a review and synthesis. Mar. Pollut. Bull. 158, 111398.
He, B., Wijesiri, B., Ayoko, G.A., Egodawatta, P., Rintoul, L., Goonetilleke, A., 2020. Influential factors on microplastics occurrence in river sediments. Sci. Total Environ. 738, 139901.

He, B.B., Smith, M., Egodawatta, P., Ayoko, G.A., Rintoul, L., Goonetilleke, A., 2021. Dispersal and transport of microplastics in river sediments. Environ. Pollut. 279.

Hengstmann, E., Weil, E., Wallbott, P.C., Tamminga, M., Fischer, E.K., 2021. Microplastics in lakeshore and lakebed sediments - external influences and temporal and spatial variabilities of concentrations. Environ. Res. 197, 111141.

Hidalgo-Ruz, V., Gutow, L., Thompson, R.C., Thiel, M., 2012. Microplastics in the marine environment: a review of the methods used for identification and quantification. Environ. Sci. Technol. 46, 3060–3075.

Ho, N.H.E., Not, C., 2019. Selective accumulation of plastic debris at the breaking wave area of coastal waters. Environ. Pollut. 245, 702–710.

Horton, A.A., Walton, A., Spurgeon, D.J., Lahive, E., Svendsen, C., 2017. Microplastics in freshwater and terrestrial environments: evaluating the current understanding to identify the knowledge gaps and future research priorities. Sci. Total Environ. 586, 127–141.

Hu, D., Zhang, Y., Shen, M., 2020. Investigation on microplastic pollution of Dongting Lake and its affiliated rivers. Mar. Pollut. Bull. 160, 111555.

Huang, Z.Q., 2018. A Study on the Spatial Production of Tibetan Community in the Lakeside District of Qinghai Lake under the Influence of Tourism - Taking Heimahe Community as an Example. Qinghai Normal University.

Imhof, H.K., Ivleva, N.P., Schmid, J., Niessner, R., Laforsch, C., 2013. Contamination of beach sediments of a subalpine lake with microplastic particles. Curr. Biol. 23, R867–R868.

Imhof, H.K., Sigl, R., Brauer, E., Feyl, S., Giesemann, P., Klink, S., Leupolz, K., Loder, M.G., Loschel, L.A., Missun, J., Muszynski, S., Ramsperger, A.F., Schrank, I., Speck, S., Steibl, S., Trotter, B., Winter, I., Laforsch, C., 2017. Spatial and temporal variation of macro-, meso- and microplastic abundance on a remote coral island of the Maldives, Indian Ocean. Mar. Pollut. Bull. 116, 340–347.

Ivar do Sul, J.A., Costa, M.F., 2014. The present and future of microplastic pollution in the marine environment. Environ. Pollut. 185, 352–364.

Jian, Y., Zhang, X., Li, X., Schou, C., Charalambidou, I., Ma, L., Karanis, P., 2021. Occurrence of Cryptosporidium and Giardia in wild birds from Qinghai Lake on the Qinghai-Tibetan Plateau,China. Parasitol. Res. 120, 615–628.

Jiang, C.B., Yin, L.S., Wen, X.F., Du, C.Y., Wu, L.X., Long, Y.N., Liu, Y.Z., Ma, Y., Yin, Q.D., Zhou, Z.Y., Pan, H.M., 2018. Microplastics in sediment and surface water of West Dongting Lake and South Dongting Lake: abundance, source and composition. Int. J. Environ. Res. Public Health 15.

Jiang, C., Yin, L., Li, Z., Wen, X., Luo, X., Hu, S., Yang, H., Long, Y., Deng, B., Huang, L., Liu, Y., 2019. Microplastic pollution in the rivers of the Tibet Plateau. Environ. Pollut. 249, 91–98.

Jiang, Y., Zhao, Y., Wang, X., Yang, F., Chen, M., Wang, J., 2020. Characterization of microplastics in the surface seawater of the South Yellow Sea as affected by season. Sci. Total Environ. 724, 138375.

Ju, J., Zhu, L., Feng, J., Wang, J., Wang, Y., Xie, M., Peng, P., Zhen, X., Lü, X., 2012. Hydrodynamic process of Tibetan Plateau lake revealed by grain size: case study of Pumayum Co. Chin. Sci. Bull. 57, 2433–2441.

Kanhai, D.K., Gardfeldt, K., Lyashevska, O., Hassellov, M., Thompson, R.C., O'Connor, I., 2018. Microplastics in sub-surface waters of the Arctic Central Basin. Mar. Pollut. Bull. 130, 8–18.

Kedzierski, M., Villain, J., Falcou-Prefol, M., Kerros, M.E., Henry, M., Pedrotti, M.L., Bruzaud, S., 2019. Microplastics in Mediterranean Sea: a protocol to robustly assess contamination characteristics. PLoS One 14, e0212088.

Khatmullina, L., Isachenko, I., 2017. Settling velocity of microplastic particles of regular shapes. Mar. Pollut. Bull. 114, 871–880.

Lanzhou Institute of Geology, C., Institute of Hydrobiology, C., Institute of Microbiology, C., 1979. An Reported on Comprehensive Exploration of Qinghai Lake. Science Press, Beijing.

Lenaker, P.L., Baldwin, A.K., Corsi, S.R., Mason, S.A., Reneau, P.C., Scott, J.W., 2019. Vertical distribution of microplastics in the water column and surficial sediment from the Milwaukee River Basin to Lake Michigan. Environ. Sci. Technol. 53, 12227–12237.

Li, X.-Y., Xu, H.-Y., Sun, Y.-L., Zhang, D.-S., Yang, Z.-P., 2006. Lake-level change and water balance analysis at Lake Qinghai, West China during recent decades. Water Resour. Manag. 21, 1505–1516.

Li, X.Y., Ma, Y.J., Xu, H.Y., Wang, J.H., Zhang, D.S., 2009. Impact of land use and land cover change on environmental degradation in Lake Qinghai Watershed. Land Degrad. Dev. 20, 69–83.

Li, W., Zhang, Y., Wu, N., Zhao, Z., Xu, W., Ma, Y., Niu, Z., 2019. Colonization characteristics of bacterial communities on plastic debris influenced by environmental factors and polymer types in the Haihe Estuary of Bohai Bay, China. Environ. Sci. Technol. 53, 10763–10773.

Liang, T., Lei, Z., Fuad, M.T.I., Wang, Q., Sun, S., Fang, J.K., Liu, X., 2021. Distribution and potential sources of microplastics in sediments in remote lakes of Tibet, China. Sci. Total Environ. 806, 150526.

Lin, L., Zuo, L.Z., Peng, J.P., Cai, L.Q., Fok, L., Yan, Y., Li, H.X., Xu, X.R., 2018. Occurrence and distribution of microplastics in an urban river: a case study in the Pearl River along Guangzhou City,China. Sci. Total Environ. 644, 375–381.

Liu, J.Y., Zhuang, D.F., Wang, J.H., Zhou, W.C., Wu, S.X., 2014. In: <collab>National Tibetan Plateau Data, C.</collab> (Ed.), Landuse/Landcover data of the Qinghai Lake River Basin (2000). National Tibetan Plateau Data Center.

Liu, C., Zhu, L., Wang, J., Ju, J., Ma, Q., Qiao, B., Wang, Y., Xu, T., Chen, H., Kou, Q., Zhang, R., Kai, J., 2021a. In-situ water quality investigation of the lakes on the Tibetan Plateau. Sci. Bull. 66, 1727–1730.

Liu, Y., You, J., Li, Y., Zhang, J., He, Y., Breider, F., Tao, S., Liu, W., 2021b. Insights into the horizontal and vertical profiles of microplastics in a river emptying into the sea affected by intensive anthropogenic activities in Northern China. Sci. Total Environ. 779, 146589.

Mao, R., Song, J., Yan, P., Ouyang, Z., Wu, R., Liu, S., Guo, X., 2021. Horizontal and vertical distribution of microplastics in the Wuliangsuhai Lake sediment, northern China. Sci. Total Environ. 754, 142426.

Martin, J., Lusher, A., Thompson, R.C., Morley, A., 2017. The deposition and accumulation of microplastics in marine sediments and bottom water from the Irish Continental Shelf. Sci. Rep. 7, 10772.

Mason, S.A., Kammin, L., Eriksen, M., Aleid, G., Wilson, S., Box, C., Williamson, N., Riley, A., 2016. Pelagic plastic pollution within the surface waters of Lake Michigan, USA. J. Great Lakes Res. 42, 753–759.

Mason, S.A., Daily, J., Aleid, G., Ricotta, R., Smith, M., Donnelly, K., Knauff, R., Edwards, W., Hoffman, M.J., 2020. High levels of pelagic plastic pollution within the surface waters of Lakes Erie and Ontario. J. Great Lakes Res. 46, 277–288.

Masura, J., Baker, J., Foster, G., Courtney, A., 2015. Laboratory Methods for the Analysis of Microplastics in the Marine Environment: Recommendations for Quantifying Synthetic Particles in Waters and Sediments. NOAA Tech. Memo. NOS-OR&R-4. 39.

Min, K., Cuiffi, J.D., Mathers, R.T., 2020. Ranking environmental degradation trends of plastic marine debris based on physical properties and molecular structure. Nat. Commun. 11, 727.

O'Bryan, D.M., Xie, Z., Wang, Y., Du, J., Brauner, C.J., Richards, J.G., Wood, C.M., Chen, X.Q., Murray, B.W., 2010. Phylogeography and conservation genetics of Lake Qinghai scaleless carp Gymnocypris przewalskii. J. Fish Biol. 77, 2072–2092.

Pazos, R.S., Bauer, D.E., Gomez, N., 2018. Microplastics integrating the coastal planktonic community in the inner zone of the Rio de la Plata estuary (South America). Environ. Pollut. 243, 134–142.

PlasticEurope, 2019. Plastics - The Facts 2019. https://www.plasticseurope.org.

Pohl, F., Eggenhuisen, J.T., Kane, I.A., Clare, M.A., 2020. Transport and burial of microplastics in deep-marine sediments by turbidity currents. Environ. Sci. Technol. 54, 4180–4189.

Qi, Y., Wang, W., Zhou, S.X., Lu, S.J., 2015. Temporal and spatial variation of total nitrogen, total phosphorus and dissolved oxygen in the Qinghai Lake Jiangsu. Agric. Sci. 43, 357–359 (in Chinese).

Quesadas-Rojas, M., Enriquez, C., Valle-Levinson, A., 2021. Natural and anthropogenic effects on microplastic distribution in a hypersaline lagoon. Sci. Total Environ. 776, 145803.

Raju, S., Carbery, M., Kuttykattil, A., Senthirajah, K., Lundmark, A., Rogers, Z., Scb, S., Evans, G., Palanisami, T., 2020. Improved methodology to determine the fate and transport of microplastics in a secondary wastewater treatment plant. Water Res. 173, 115549.

Rezaei, M., Riksen, M.J.P.M., Sirjani, E., Sameni, A., Geissen, V., 2019. Wind erosion as a driver for transport of light density microplastics. Sci. Total Environ. 669, 273–281.

Rodrigues, M.O., Abrantes, N., Goncalves, F.J.M., Nogueira, H., Marques, J.C., Goncalves, A.M.M., 2018. Spatial and temporal distribution of microplastics in water and sediments of a freshwater system (Antua River, Portugal). Sci. Total Environ. 633, 1549–1559.

Sarkar, D.J., Das Sarkar, S., Das, B.K., Manna, R.K., Behera, B.K., Samanta, S., 2019. Spatial distribution of meso and microplastics in the sediments of river Ganga at eastern India. Sci. Total Environ. 694, 133712.

Scopetani, C., Chelazzi, D., Cincinelli, A., Esterhuizen-Londt, M., 2019. Assessment of microplastic pollution: occurrence and characterisation in Vesijarvi lake and Pikku Vesijarvi pond,Finland. Environ. Monit. Assess. 191, 652.

Scopetani, C., Esterhuizen-Londt, M., Chelazzi, D., Cincinelli, A., Setala, H., Pflugmacher, S., 2020. Self-contamination from clothing in microplastics research. Ecotoxicol. Environ. Saf. 189, 110036.

Sha, Z., Wang, Q., Wang, J., Du, J., Hu, J., Ma, Y., Kong, F., Wang, Z., 2017. Regional environmental change and human activity over the past hundred years recorded in the sedimentary record of Lake Qinghai,China. Environ. Sci. Pollut. Res. 24, 9662–9674.

Song, C., Huang, B., Ke, L., Richards, K.S., 2014. Seasonal and abrupt changes in the water level of closed lakes on the Tibetan Plateau and implications for climate impacts. J. Hydrol. 514, 131–144.

Statistics, 2020. Qinghai Statistical Yearbook. China Statistic Publishing House, Xining.

Sun, X., Wang, T., Chen, B., Booth, A.M., Liu, S., Wang, R., Zhu, L., Zhao, X., Qu, K., Bin, X., 2020. Factors influencing the occurrence and distribution of microplastics in coastal sediments: from source to sink. J. Hazard. Mater. 410, 124982.

Thushari, G.G.N., Senevirathna, J.D.M., Yakupitiyage, A., Chavanich, S., 2017. Effects of microplastics on sessile invertebrates in the eastern coast of Thailand: an approach to coastal zone conservation. Mar. Pollut. Bull. 124, 349–355.

Tibbetts, J., Krause, S., Lynch, I., Smith, G.H.S., 2018. Abundance, distribution, and drivers of microplastic contamination in urban river environments. Water 10.

Turner, S., Horton, A.A., Rose, N.L., Hall, C., 2019. A temporal sediment record of microplastics in an urban lake, London,UK. J. Paleolimnol. 61, 449–462.

Uddin, S., Fowler, S.W., Uddin, M.F., Behbehani, M., Naji, A., 2021. A review of microplastic distribution in sediment profiles. Mar. Pollut. Bull. 163, 111973.

Uurasjarvi, E., Paakkonen, M., Setala, O., Koistinen, A., Lehtiniemi, M., 2021. Microplastics accumulate to thin layers in the stratified Baltic Sea. Environ. Pollut. 268, 115700.

Van Cauwenberghe, L., Devriese, L., Galgani, F., Robbens, J., Janssen, C.R., 2015. Microplastics in sediments: a review of techniques, occurrence and effects. Mar. Environ. Res. 111, 5–17.

Vaughan, R., Turner, S.D., Rose, N.L., 2017. Microplastics in the sediments of a UK urban lake. Environ. Pollut. 229, 10–18.

Vermeiren, P., Munoz, C.C., Ikejima, K., 2016. Sources and sinks of plastic debris in estuaries: a conceptual model integrating biological, physical and chemical distribution mechanisms. Mar. Pollut. Bull. 113, 7–16.

Vianello, A., Boldrin, A., Guerriero, P., Moschino, V., Rella, R., Sturaro, A., Da Ros, L., 2013. Microplastic particles in sediments of Lagoon of Venice, Italy: first observations on occurrence, spatial patterns and identification. Estuar. Coast. Shelf Sci. 130, 54–61.

Wang, X., Yang, H., Gong, P., Zhao, X., Wu, G., Turner, S., Yao, T., 2010. One century sedimentary records of polycyclic aromatic hydrocarbons, mercury and trace elements in the Qinghai Lake, Tibetan Plateau. Environ. Pollut. 158, 3065–3070.

Wang, C., Wang, H., Song, G., Zheng, M., 2018. Grain size of surface sediments in Selin Co (central Tibet) linked to water depth and offshore distance. J. Paleolimnol. 61, 217–229.

Wang, C., Xing, R., Sun, M., Ling, W., Shi, W., Cui, S., An, L., 2020. Microplastics profile in a typical urban river in Beijing. Sci. Total Environ. 743, 140708.

Wong, J.K.H., Lee, K.K., Tang, K.H.D., Yap, P.S., 2020. Microplastics in the freshwater and terrestrial environments: prevalence, fates, impacts and sustainable solutions. Sci. Total Environ. 719, 137512.

Wright, S.L., Thompson, R.C., Galloway, T.S., 2013. The physical impacts of microplastics on marine organisms: a review. Environ. Pollut. 178, 483–492.

Wu, M.T., 2018. All-for-one Tourism "Multi-point Blooming" Famous Scenic Spots Continue to be Popular, and Niche Tourism Is Highly Sought After. Xihai Metropolis Daily.

Wu, K.N., Zhao, R., 2019. Soil texture classification and its application in China. Acta Pedol. Sin. 56, 227–241.

Wu, Q.C., Hu, Q., Gao, Q.X., 2006. Environmental Pollution Status and Treatment Suggestions in Qinghai Lake Basin. Symposium on Lake Protection and Sustainable Development of Qinghai Lake2006.

Xiong, X., Zhang, K., Chen, X.C., Shi, H.H., Luo, Z., Wu, C.X., 2018. Sources and distribution of microplastics in China's largest inland lake - Qinghai Lake. Environ. Pollut. 235, 899–906.

Xu, H., Liu, X., An, Z., Hou, Z., Dong, J., Liu, B., 2010. Spatial pattern of modern sedimentation rate of Qinghai Lake and a preliminary estimate of the sediment flux. Chin. Sci. Bull. 55, 621–627.

Yang, Y., Wang, L., Han, J., Tang, X., Ma, M., Wang, K., Zhang, X., Ren, Q., Chen, Q., Qiu, Q., 2015. Comparative transcriptomic analysis revealed adaptation mechanism of Phrynocephalus erythrurus, the highest altitude lizard living in the Qinghai-Tibet Plateau. BMC Evol. Biol. 15, 101.

Yang, L., Luo, W., Zhao, P., Zhang, Y., Kang, S., Giesy, J.P., Zhang, F., 2021a. Microplastics in the Koshi River, a remote alpine river crossing the Himalayas from China to Nepal. Environ. Pollut. 290, 118121.

Yang, L., Zhang, Y., Kang, S., Wang, Z., Wu, C., 2021b. Microplastics in freshwater sediment: a review on methods, occurrence, and sources. Sci. Total Environ. 754, 141948.

Yin, L., Wen, X., Du, C., Jiang, J., Wu, L., Zhang, Y., Hu, Z., Hu, S., Feng, Z., Zhou, Z., Long, Y., Gu, Q., 2020. Comparison of the abundance of microplastics between rural and urban areas: a case study from East Dongting Lake. Chemosphere 244, 125486.

Yonkos, L.T., Friedel, E.A., Perez-Reyes, A.C., Ghosal, S., Arthur, C.D., 2014. Microplastics in four estuarine rivers in the Chesapeake Bay, U.S.A. Environ. Sci. Technol. 48, 14195–14202.

Yuan, W., Liu, X., Wang, W., Di, M., Wang, J., 2019. Microplastic abundance, distribution and composition in water, sediments, and wild fish from Poyang Lake,China. Ecotoxicol. Environ. Saf. 170, 180–187.

Zhang, H., 2017. Transport of microplastics in coastal seas. Estuar. Coast. Shelf Sci. 199, 74–86.

Zhang, K., Su, J., Xiong, X., Wu, X., Wu, C., Liu, J., 2016. Microplastic pollution of lakeshore sediments from remote lakes in Tibet plateau, China. Environ. Pollut. 219, 450–455.

Zhang, K., Shi, H., Peng, J., Wang, Y., Xiong, X., Wu, C., Lam, P.K.S., 2018. Microplastic pollution in China's inland water systems: a review of findings, methods, characteristics, effects, and management. Sci. Total Environ. 630, 1641–1653.

Zhang, J., Wang, L., Kannan, K., 2021a. Quantitative analysis of polyethylene terephthalate and polycarbonate microplastics in sediment collected from South Korea, Japan and the USA. Chemosphere 279, 130551.

Zhang, Q., Liu, T., Liu, L., Fan, Y., Rao, W., Zheng, J., Qian, X., 2021b. Distribution and sedimentation of microplastics in Taihu Lake. Sci. Total Environ. 795, 148745.

Zobkov, M., Belkina, N., Kovalevski, V., Zobkova, M., Efremova, T., Galakhina, N., 2020. Microplastic abundance and accumulation behavior in Lake Onego sediments: a journey from the river mouth to pelagic waters of the large boreal lake. J. Environ. Chem. Eng. 8.

SUPPORTING INFORMATION

Distribution of microplastics in benthic sediments of Qinghai Lake on the Tibetan Plateau, China

Ning Jiang[a, b], Wei Luo[a, b, c*], Pin Zhao[a, b], Bila Ga[a, b], Junmei Jia[d], John P. Giesy[e, f, g, h]

a *Laboratory of Solid Waste Treatment and Recycling, Research Center for Eco-Environmental Sciences, Chinese Academy of Sciences, Beijing 100085, China*

b *University of Chinese Academy of Sciences, Beijing 100049, China*

c *State Key Laboratory of Urban and Regional Ecology Research Center for Eco-Environmental Sciences, Chinese Academy of Sciences, Beijing 100085, China*

d *State Key Laboratory of Plateau Ecology and Agriculture, Qinghai University, Xining, 810016, China*

e *Toxicology Program Faculty, Toxicology Centre, University of Saskatchewan, Saskatoon SK S7N 5B3, Canada*

f *Department of Veterinary Biomedical Sciences, University of Saskatchewan, Saskatoon, SK, Canada*

g *Department of Integrative Biology, Michigan State University, East Lansing, MI, USA*

h *Department of Environmental Science, Baylor University, Waco, TX, USA*

* Corresponding author.

E-mail addresses: luow@rcees.ac.cn

Supplementary caption

Text S1 Extraction of microplastics

Text S2 Procedures of blank tests

Test S3 Sampling method of surface sediments in lake

Table S1 Comparison of abundances and characteristics of microplastics in lake sediments worldwide

Table S2 Spearman's rank correlation between microplastic abundances in sediments and environment parameters in Qinghai Lake

Table S3 Numbers and characters of microplastics in samples from each site

Text S1 Extraction of microplastics

All sediment samples were analyzed by following four steps according to a modified procedure proposed by the NOAA (Masura et al., 2015). They were dried at 60 °C for at least 48 h and homogenized by stirring with a stainless-steel spoon. Two duplicates of 50g of each dried sediment samples were transferred to 800 mL glass flasks and mixed with 300 mL of $ZnCl_2$ solution (density 1.6 g cm^{-3}) and shaken 15 min and left overnight for sedimentation. The solution was decanted. The supernatant, which contained the MP items, was filtered through a stainless-steel sieve with a mesh size of 50 μm. The residual solids on the sieve were transferred to a clean beaker using a small amount of distilled water. The extraction was repeated three times for each sample to increase recovery efficiency. 20 mL of a 0.05 M Fe (II) solution in acidic medium (0.1 M H_2SO_4) and 20 mL of 30% H_2O_2 were added until all the organic substances were digested. The digested samples were vacuum filtered through a nylon filter (20 μm pore size) which was washed with $ZnCl_2$ solution (1.6 g cm^{-3}). The resulting eluent settled for 24 h in a separatory funnel. The MP particles floated, while inorganic materials (sand, metal, and glass) sedimented and were drained from the funnel. The remaining sample was filtered through a cellulose acetate filter (0.45 μm pore size) which was then dried at room temperature in Petri dishes and stored until characterization with appropriate techniques.

Text S2 Procedures of blank tests

Field and laboratory blanks were collected to account for potential contamination of samples during the collection and processing stages. Two field blanks were collected during sampling trip. Field blanks were taken by placing ~30 g of anhydrous sodium sulphate in 250-ml glass jars and leaving them open to air until the sediment sample was collected. Feld blanks were processed using the same protocol as for sediment samples. Ultrapure water blank was processed concurrently to field blank processing. Each field blank was corrected for the ultrapure water blank by color-category. Two laboratory blanks were processed and analyzed concurrently with samples to account for potential of airborne contamination during processing. Laboratory blanks consisted of ultrapure water in a glass beaker remaining open to air during the processing of a single sample. After processing lab blanks, it was determined that field blank numbers were very low (one blue fiber total) and within the error of the lab blanks, and so field blanks were not included in the blank correction. Particles in all blanks consisted of 100% microfibers, thus only microfibers concentrations were blank corrected by subtracting based on color (Adams et al., 2021).

Test S3 Sampling method of surface sediments in lake

Sediment samples were collected from a small wooden boat, using stainless-steel grab sampler with a square opening of 15 cm × 15 cm at its bottom. The top of the sampler was attached to a 50 m long yellow rope made of flax fibers. Two randomly selected aeras of 15 cm × 15 cm at each site, which were not more than 10 m apart, were sampled using the sampler. Immediately upon retrieval, sediment was transferred from the sampler to a stainless-steel pan where a stainless-steel spatula was used to collect the upper 0~5 cm of sediment. Items >5 mm in the sample were removed, measured and recorded. Two samples of at least 500 g collected at each site were thoroughly mixed, and then about 1 kg of the mixed sample was transferred to a labeled aluminum container with a cover. All samples were delivered to a lab as quickly as possible and stored at −20 °C until further analysis (Cincinelli et al., 2021; Liang et al., 2021).

Table S1 Comparison of abundances and characteristics of microplastics in lake sediments worldwide

Rural/urban area	Name and location	Method (Extraction Liquid)	Abundance (items/kg, dm)	Size	Shape	Color	Polymer types	References
Rural area	Qinghai lake, China	benthic, $ZnCl_2$ (1.6 g cm^{-3})	393±457 (60-1150)	<0.5 mm dominant	Fiber (82.91%), Fragment, (16.55%), Film (11.92%), Foam, Sphere;	Transparent (52.36%), Blue (21.64%), Green, Other	PP, PA, PET	This study
	Twelve remote lakes in the north of the Tibet, China	Shoreline, $ZnCl_2$ (1.5 g cm^{-3})	545±298 (17-2644)	0.05–0.5 mm (53.14%)	Fiber (85.59%), film (7.91%), fragment (6.50%)	Black (51.65%), transparent (27.78%), blue (14.64%), red (5.93%)	PA (55.97%), PET (33.77%)	(Liang et al., 2021)
	Lakes Mead and Mohave, USA	benthic, lithium metatungstate (1.6 g/cm^{-3})	88-1010	0.355-1mm (63.7%)	Fiber (80.3%), fragment (8.9%), film (7.7%), foam (1.4%), other (1.7%)	clear (37.8% average), black (26.2%), blue (24.3%), and red (6.5%)	N. A	(Baldwin et al., 2020)
	Lake Bolsena and Chiusi, Italy	Shoreline, NaCl (1.2 g cm^{-3})	Lake Bolsena: 112±32 Lake Chiusi: 234±85	<0.5mm	Fiber dominant	N. A	N. A	(Fischer et al., 2016)
	The black sea	Benthic, NaCl	106.7 (0-390)	N. A	Fiber dominant	black, blue and clear/transparent	PE/PP (44.5%), PA (32.0%), other (23.5%)	(Cincinelli et al., 2021)
Urbanization area	Dishui Lake in Shanghai, China	Shoreline, NaCl (1.2 g cm^{-3})	46 (ALS site)-230 (TCS site)	1–5 mm (91%) domimamt	Sheet (53%), Line (22%)	White (54%) and blue (30%) dominant	PP (69%), PS (12%), PE (8%)	(Liu and Fang, 2020)
	Eighteen different trophic state lakes, China	Benthic, NaCl (1.2 g cm^{-3})	219 (90-580)	<1 mm (70%) was the most abundant	Fiber (94.77%),	Blue (69.11%)	PP (10-80%), PE (8%), PC	(Li et al., 2019)
	West Dongting Lake and South Dongting Lake, China	Shoreline and benthic, $ZnCl_2$ (1.5 g cm^{-3})	West Dongting Lake 388.57 ± 66.19, South Dongting Lake 501.43 ± 331.18 (200 - 1150)	<0.5 mm	Fiber dominant (12.17-77.42%)	Transparent dominant	PET (50%)	(Jiang et al., 2018)
	East Dongting Lake, China	Shoreline, $ZnCl_2$ (1.5 g cm^{-3})	403 (180-693)	<0.5 mm	Fiber dominant (41.49-100%), fragment (3.57-50%)	Transparent dominant (23.4-67.86%)	PET (29.55%), PA (19.32%), PE (15.91%), PP (12.5%), PS (6.82%)	(Yin et al., 2020)
	Dongting lake, China	Benthic, NaCl /$ZnCl_2$ (1:3) (1.5	385 ± 69.6 (210-520)	<1 mm	Fiber dominant (50-91%)	N. A	PE (28.2%), PP (17.9%), PET (12.8%), PVC (10.3%),	(Hu et al., 2020)

	g cm^{-3})					PA (10.3%), other (20.5%)	
Five reed farms around East Dongting Lake, China	Shoreline, $ZnCl_2$ (1.5 g cm^{-3})	511.2±295.0 (125.7-1219.5)	<0.5 mm (63%)	Fiber dominant (89%)	Transparent (58%)	PE (29.4%), PA (24.8%), PET (15.6%), PP (11.9%), PS (9.2%)	(Yin et al., 2021)
Wuliangsuhai Lake, China	Benthic, $ZnCl_2$ (1.5 g cm^{-3})	453±201 (165-724)	0-0.5mm (42-57%)	Fiber dominant (more than 40%)	N. A	PS (27.3%), PET (12.5%), PVC (7%)	(Mao et al., 2021)
Poyang Lake, China	Benthic, NaCl (1.2 g cm^{-3})	161 (54-506)	0.1-0.5mm	Fiber dominant (44.1%)	Colored (36.6%)	PP (38.5%), PE (25.7%), PVC (11.4%)	(Yuan et al., 2019)
Taihu Lake, China	Benthic, NaCl (1.2 g cm^{-3})	893 (464-1381)	N. A	Fiber and fragment dominant	N. A	PE and PP	(Zhang et al., 2021)
Lakes in Changsha, China	Shoreline, $ZnCl_2$ (1.5 g cm^{-3})	512 (270.17± 48.23 -866.59± 37.96)	<1mm	Fragment (50.82%), fiber (28.15%), film (18.14%)	Transparent dominant	PS (29.41%), PE (19.12%), PET (14.71%), PP, PA, PVC	(Wen et al., 2018)
Lake Onego in Europe	Benthic, HCOOK (1.5 g cm^{-3})	2188.7 ± 1164.4	N. A	Fiber (54.6%), beads (19.6%), films (12.9%), fragment (12.9%)	Transparent (45.3%), blue (16.9%) and beige (13.3%)	Polycarbonate, polyethylene, cellophane and polyacrylonitrile were the most abundant polymers (57%)	(Zobkov et al., 2020)
The lagoon of Bizerte, Tunisia	Shoreline, NaCl (1.2 g cm^{-3})	7960 ± 6840 (3000-18,000)	0.3-5 mm	Fiber and fragment dominant	Transparent (most abundant), white, blue, red, and green	N. A	(Abidli et al., 2017)
Lake Ontario, Canada	Shoreline, sodium polytungstate (1.5 g cm^{-3})	760 (20 -27830)	<2 mm	Fiber and fragment dominant (12.17-77.42%)	N. A	PE (31%), PS (10%), PU (4%),	(Ballent et al., 2016)
Lake Simcoe in Ontario, Canada	Benthic, $CaCl_2$ (1.4 g cm^{-3})	372 (8.3-1070)	N. A	Fibers (89.2%),	Transparent (46.7%), black (20.8%), red (11.7%)	PE (41%), PP (22%)	(Felismino et al., 2021)
Vembanad Lake, India	Benthic, NaCl (1.3 g cm^{-3})	253 (96-496)	N. A	Film and foam dominant	N. A	PE (26-91%)	(Sruthy and Ramasamy, 2017)
Vesijärvi Lake, Finland	Benthic, NaCl (1.2 g cm^{-3})	395.8 ± 90.7	N. A	Fiber dominant	N. A	PA (53.3%), CE (33.3%), PS (6.7%), PU-PET (6.7%)	(Scopetani et al., 2019)
Red Hills Lake, India	Benthic, NaCl (1.2 g cm^{-3})	27	<1mm	Fibers (37.9%) dominant	White (65%) dominant	PP and PE	(Gopinath et al., 2020)
Ox- Bow Lake, Nigeria	Benthic, Sodium Iodide (1.6 g cm^{-3})	raining season: 507-7593 dry season: 347-4031	N. A	Fiber dominant	Red dominant	raining season: PVC (81.5%) dry season: PVC (72.6%)	(Oni et al., 2020)
Veeranam lake, India	Benthic, $ZnCl_2$ (1.5 g cm^{-3})	309 (92-604)	0.3-1mm (47%)	N. A	White (48%), red (21%), black (15%),	Nylon (37.92%) predomiant	(Bharath et al., 2021)

						green (9%), blue (5%) and yellow (2%)		
	Hampstead No. 1 Pond in London, UK	Sediment core, sodium polytungstate (2.1 g cm^{-3})	539	500-µm to 1 mm dominant	>80% fiber	Blue 25%, white 22%, Red 17%	PS, PA	(Turner et al., 2019)
	Ontario shoreline of Lake Erie, Canada	Shoreline, sodium polytungstate (1.5 g cm^{-3})	(0-391)	N. A	Fiber (64%), fragment (36%)	Blue and black	PE, PP, PS, PVC	(Dean et al., 2018)

Table S2 Spearman's rank correlation between microplastic abundances in sediments and environment parameters in Qinghai Lake

	Abundance	Depth	Distance	Conductivity	Salinity	Turbidity	Clay (<2 um)	Silt (2-20 μm)	Sand (20-2000 μm)
Abundance	1								
Depth	-0.63[a]	1							
Distance	-0.74[b]	0.70[b]	1						
Conductivity	-0.71[b]	0.71[b]	0.85[b]	1					
Salinity	-0.58[a]	0.65[a]	0.86[b]	0.81[b]	1				
Turbidity	0.59[a]	-0.61[a]	-0.88[b]	-0.86[b]	-0.91[b]	1			
Clay (<2 um)	-0.76[b]	0.71[b]	0.71[b]	0.63[a]	0.53	-0.60[a]	1		
Silt (2-20 μm)	-0.63[a]	0.77[b]	0.56[a]	0.52	0.63[a]	-0.53[a]	0.78[b]	1	
Sand (20-2000 μm)	0.71[b]	-0.73[b]	-0.64[a]	-0.58[a]	-0.60[a]	0.59[a]	-0.90[b]	-0.93[b]	1

[a] Correlation is significant at the 0.05 level.

[b] Correlation is significant at the 0.01 level.

Table S3 Numbers and characters of microplastics in samples from each site

Sampling site	Sediment dry weight (g)	Sample ID	Shape	Color	Size (μm)
E1-1	50.10	1	fiber	green	72
		2	fragment	transparent	785
		3	fiber	red	491
		4	fiber	green	664
		5	fiber	blue	2680
		6	fiber	green	148
		7	fiber	green	106
		8	fiber	green	272
		9	fiber	green	449
		10	fragment	blue	167
E1-2	50.38	11	fiber	black	250
		12	fiber	other	213
		13	fiber	transparent	589
		14	fiber	green	245
		15	fiber	green	232
		16	fiber	yellow	442
		17	fiber	green	668
		18	fiber	green	214
		19	fragment	red	117
		20	fiber	green	7140
		21	fiber	green	169
		22	fiber	green	256
		23	fiber	green	151
		24	fiber	blue	215
		25	fiber	green	1680
E2-1	50.08	26	fiber	transparent	638
		27	fiber	transparent	453
		28	fiber	transparent	249
		29	fiber	transparent	762
		30	fiber	transparent	632
		31	fiber	green	6380
		32	fiber	transparent	232
		33	fiber	transparent	3030

		34	fragment	blue	155
		35	fiber	transparent	918
		36	fiber	transparent	184
		37	fiber	transparent	906
		38	fiber	transparent	367
		39	fiber	yellow	1070
		40	fiber	black	1250
		41	fiber	blue	477
		42	fiber	red	1390
		43	fiber	transparent	459
		44	fiber	transparent	990
		45	fiber	red	476
		46	fiber	blue	415
		47	fragment	transparent	235
		48	fiber	blue	696
		49	fiber	transparent	461
		50	fiber	blue	209
		51	fiber	transparent	487
		52	fiber	blue	1010
		53	fiber	red	1340
		54	fiber	transparent	9360
		55	fiber	green	732
		56	fiber	red	3090
		57	fiber	blue	524
		58	fiber	blue	350
		59	fiber	green	4010
		60	fiber	transparent	485
		61	fiber	green	1990
		62	fiber	transparent	1220
		63	fiber	blue	326
		64	fiber	transparent	405
		65	fiber	green	660
		66	fiber	transparent	2500
		67	fiber	transparent	643
		68	fiber	transparent	1420
		69	fiber	blue	229
		70	fiber	transparent	176

		71	fiber	black	439
		72	fiber	blue	425
		73	fiber	blue	639
		74	fiber	transparent	1660
		75	fiber	transparent	2890
		76	fiber	red	2620
		77	fiber	transparent	848
		78	fiber	transparent	1110
		79	fiber	blue	230
		80	fiber	yellow	771
		81	fiber	transparent	531
		82	fiber	blue	203
		83	fiber	transparent	352
		84	fragment	transparent	250
E2-2	50.33	85	fiber	blue	391
		86	fiber	black	1370
		87	fiber	green	736
		88	fiber	blue	1570
		89	fiber	transparent	220
		90	fiber	transparent	390
		91	fragment	transparent	318
		92	fiber	blue	781
		93	fragment	red	211
		94	fiber	transparent	1930
		95	fiber	black	154
		96	fiber	transparent	310
		97	fiber	transparent	333
		98	fiber	transparent	921
		99	fiber	yellow	1900
		100	fiber	black	853
		101	fiber	transparent	938
		102	fiber	transparent	245
		103	fiber	transparent	363
		104	fiber	transparent	174
		105	fiber	red	2010
		106	fiber	blue	418
		107	fiber	transparent	447

		108	fiber	transparent	159
		109	fiber	transparent	4950
		110	fiber	transparent	303
		111	fragment	transparent	117
		112	fiber	transparent	470
		113	fiber	transparent	1040
		114	fiber	transparent	618
		115	fiber	blue	683
		116	fiber	transparent	168
		117	fiber	blue	586
		118	fragment	blue	328
		119	fiber	transparent	786
		120	fiber	other	594
		121	fiber	red	1120
		122	fiber	transparent	346
		123	fiber	blue	295
		124	fiber	transparent	3600
		125	fiber	transparent	243
		126	fiber	blue	715
		127	fiber	transparent	394
		128	fiber	green	259
		129	fiber	transparent	182
		130	fragment	blue	65
		131	fiber	green	752
		132	fiber	transparent	759
		133	fiber	transparent	323
		134	fiber	blue	645
E3-1	49.80	135	fragment	green	224
		136	fiber	blue	91
		137	fragment	blue	72
		138	fiber	transparent	422
		139	fragment	blue	102
		140	fragment	other	183
		141	fiber	blue	991
		142	fiber	green	2140
		143	fiber	blue	1230
		144	fiber	transparent	590

		145	fragment	transparent	309
		146	fiber	transparent	288
		147	fiber	transparent	890
		148	fragment	blue	133
		149	fiber	transparent	680
		150	fiber	transparent	455
		151	fiber	transparent	1040
		152	fiber	transparent	800
		153	fiber	blue	153
		154	fiber	black	361
		155	fiber	transparent	225
		156	fiber	blue	118
		157	fiber	blue	522
		158	fiber	transparent	834
		159	fiber	transparent	354
		160	fiber	transparent	200
		161	fiber	transparent	217
		162	fiber	transparent	3120
		163	fiber	transparent	176
		164	fragment	transparent	164
		165	fiber	transparent	252
		166	fiber	transparent	165
		167	fiber	transparent	221
		168	fragment	transparent	1090
		169	fiber	transparent	930
		170	fiber	transparent	652
		171	fragment	blue	85
		172	fragment	blue	64
		173	fiber	transparent	438
		174	fiber	transparent	134
E3-2	50.19	175	fiber	transparent	542
		176	fragment	green	111
		177	fragment	transparent	238
		178	fragment	green	66
		179	pellet	other	157
		180	fragment	blue	76
		181	fiber	transparent	540

		182	fiber	transparent	517
		183	film	transparent	440
		184	fiber	transparent	234
		185	fiber	red	2210
		186	fragment	blue	176
		187	fiber	transparent	314
		188	fiber	other	1770
		189	fiber	other	502
		190	fiber	transparent	451
		191	fragment	blue	155
		192	fiber	transparent	1020
		193	fiber	black	290
		194	fiber	transparent	346
		195	fiber	transparent	261
		196	fiber	transparent	257
		197	fiber	transparent	403
		198	fiber	blue	544
		199	fiber	transparent	3070
		200	fiber	transparent	1560
		201	fragment	transparent	214
		202	fragment	transparent	189
		203	fiber	transparent	214
		204	fiber	transparent	605
		205	fiber	transparent	562
		206	fiber	transparent	888
		207	fiber	transparent	459
		208	fiber	transparent	170
		209	fragment	green	165
		210	fiber	transparent	412
		211	fiber	transparent	2920
		212	fiber	transparent	367
		213	fiber	transparent	278
		214	fragment	blue	254
		215	fiber	transparent	240
		216	fiber	transparent	171
		217	fiber	transparent	285
		218	fiber	transparent	514

		219	fragment	transparent	302
		220	fiber	transparent	923
		221	fiber	black	364
		222	fiber	transparent	1770
		223	fiber	transparent	1060
		224	fiber	transparent	1090
		225	fiber	transparent	371
		226	fiber	transparent	320
		227	fiber	transparent	579
		228	fiber	transparent	318
		229	fiber	transparent	1460
		230	fiber	transparent	762
E4-1	50.30	231	fiber	transparent	359
		232	fragment	red	58
		233	fragment	transparent	213
		234	fiber	other	179
		235	fragment	transparent	292
		236	fiber	blue	249
		237	fiber	blue	210
		238	fiber	blue	289
		239	fiber	blue	378
		240	fiber	blue	214
		241	fragment	transparent	132
		242	fiber	other	177
		243	fragment	blue	67
		244	fiber	blue	368
		245	fiber	blue	807
		246	fiber	transparent	443
		247	fiber	transparent	253
		248	fiber	blue	282
		249	fiber	transparent	219
		250	fiber	other	172
		251	fiber	transparent	513
		252	fiber	transparent	212
		253	fiber	blue	917
		254	fiber	transparent	230
		255	fiber	transparent	168

		256	fiber	transparent	161
		257	fiber	transparent	375
		258	fiber	transparent	536
		259	fiber	transparent	418
		260	fragment	white	340
		261	fiber	transparent	1940
		262	fiber	transparent	797
		263	fiber	transparent	248
		264	fiber	blue	206
		265	fragment	transparent	222
		266	fiber	transparent	376
		267	fragment	red	68
		268	fragment	white	316
		269	fiber	transparent	473
		270	fiber	other	134
		271	fiber	transparent	1320
		272	fiber	transparent	237
		273	fiber	transparent	194
		274	fragment	white	245
		275	fiber	red	457
		276	fiber	black	176
		277	fiber	transparent	534
		278	fiber	transparent	841
		279	fiber	blue	259
		280	fiber	transparent	148
		281	fiber	black	203
		282	fiber	other	417
		283	fiber	blue	125
E4-2	50.26	284	fiber	transparent	1490
		285	fragment	black	107
		286	fiber	transparent	1490
		287	fiber	other	864
		288	fiber	transparent	587
		289	fiber	transparent	942
		290	fiber	transparent	266
		291	fiber	black	331
		292	fiber	transparent	313

		293	fiber	black	302
		294	fiber	transparent	874
		295	fiber	transparent	773
		296	fiber	black	358
		297	fiber	blue	230
		298	fiber	transparent	2790
		299	fiber	transparent	643
		300	fiber	transparent	332
		301	fiber	transparent	233
		302	fiber	transparent	366
		303	fiber	transparent	280
		304	fiber	transparent	342
		305	fiber	transparent	214
		306	fiber	transparent	424
		307	fiber	transparent	282
		308	fiber	transparent	1040
		309	fiber	transparent	299
		310	fiber	transparent	427
		311	fiber	blue	3210
		312	fragment	red	460
		313	fiber	transparent	334
		314	fiber	red	1330
		315	fiber	transparent	359
		316	fiber	blue	201
		317	fiber	transparent	308
		318	fiber	transparent	682
		319	fiber	transparent	1090
		320	fiber	transparent	1190
		321	fragment	blue	78
		322	fiber	blue	611
		323	fiber	transparent	369
		324	fiber	black	437
		325	fiber	transparent	1680
		326	fiber	black	470
		327	fiber	blue	635
		328	fragment	red	2340
		329	fiber	transparent	261

		330	fiber	transparent	361
		331	fiber	transparent	162
		332	fiber	transparent	750
		333	fiber	transparent	774
		334	fiber	transparent	282
		335	fiber	transparent	291
		336	fiber	transparent	247
		337	fiber	blue	133
		338	fiber	blue	303
		339	fiber	blue	242
		340	fiber	transparent	190
		341	fiber	black	262
		342	fiber	transparent	965
		343	fiber	blue	205
		344	fiber	transparent	828
		345	fiber	blue	392
E5-1	49.99	346	fiber	transparent	272
		347	fiber	transparent	463
		348	fiber	black	1300
		349	fiber	blue	623
		350	fiber	transparent	510
		351	fiber	transparent	707
		352	fragment	green	81
		353	fragment	yellow	331
		354	fiber	blue	445
		355	fiber	blue	876
		356	fragment	black	109
E5-2	50.52	357	fiber	transparent	2330
		358	fiber	black	1560
		359	fragment	green	75
		360	fragment	other	117
		361	fiber	black	612
		362	fiber	other	125
		363	fragment	green	101
		364	fiber	blue	88
T1-1	50.16	365	fiber	blue	3070
		366	fragment	blue	623

		367	fiber	blue	260
		368	fiber	blue	1330
		369	fiber	green	294
		370	fiber	red	854
		371	fiber	transparent	2380
		372	fiber	transparent	731
		373	fiber	transparent	1050
		374	fiber	blue	364
		375	fragment	green	172
		376	fiber	black	552
		377	fragment	transparent	1060
		378	fiber	transparent	1650
		379	fiber	blue	668
		380	fiber	transparent	2070
		381	fiber	transparent	334
		382	fragment	transparent	163
		383	fiber	transparent	47
		384	fiber	transparent	1060
		385	fiber	transparent	1960
		386	fiber	transparent	607
		387	fragment	transparent	735
		388	fragment	transparent	218
		389	fiber	yellow	403
		390	fragment	green	120
		391	fiber	transparent	1050
		392	fragment	transparent	316
		393	fragment	blue	168
		394	fragment	blue	302
		395	fiber	transparent	802
		396	fiber	transparent	4520
		397	fragment	transparent	283
		398	fiber	transparent	1070
		399	fiber	transparent	1950
		400	fiber	transparent	342
		401	fiber	transparent	467
		402	fragment	red	459
		403	fiber	blue	596

		404	fragment	white	1080
		405	fiber	transparent	625
		406	fragment	green	137
		407	fiber	blue	975
		408	fiber	transparent	2940
		409	fiber	other	579
		410	fiber	transparent	1800
		411	fragment	white	372
		412	fragment	white	439
		413	fiber	transparent	1280
		414	fiber	blue	1470
		415	fragment	transparent	802
		416	fiber	blue	1020
		417	fiber	transparent	609
T1-2	50.48	418	fiber	red	1690
		419	fiber	blue	1330
		420	fiber	green	1060
		421	fiber	transparent	992
		422	fiber	blue	780
		423	fiber	blue	1150
		424	fiber	yellow	2770
		425	fiber	yellow	1650
		426	fiber	transparent	1740
		427	fiber	green	2480
		428	fiber	transparent	204
		429	fiber	red	1360
		430	fragment	white	255
		431	fragment	transparent	183
		432	fiber	red	397
		433	fiber	blue	266
		434	fiber	transparent	466
		435	fiber	transparent	919
		436	fiber	transparent	686
		437	fiber	blue	160
		438	fiber	transparent	2370
		439	fiber	red	493
		440	fiber	blue	363

		441	fragment	transparent	2020
		442	fiber	transparent	583
		443	fiber	other	980
		444	fiber	transparent	1030
		445	fiber	blue	688
		446	fragment	green	187
		447	fiber	transparent	545
		448	fragment	other	258
		449	fragment	green	203
		450	fiber	other	618
		451	fiber	blue	702
		452	fragment	transparent	1590
		453	fragment	green	202
		454	fragment	transparent	168
		455	fiber	yellow	437
		456	fiber	transparent	456
		457	fragment	transparent	272
		458	fiber	transparent	861
		459	fiber	transparent	986
		460	fragment	green	239
		461	fiber	transparent	668
		462	fiber	red	338
		463	fiber	transparent	954
		464	fiber	green	288
		465	fiber	blue	378
		466	fiber	transparent	434
		467	fiber	blue	592
		468	fiber	green	1800
		469	fiber	transparent	301
		470	fiber	transparent	2130
		471	fiber	yellow	1560
		472	fragment	green	147
		473	fiber	red	672
		474	fiber	green	2770
		475	fiber	green	1190
		476	fiber	transparent	2140
		477	fragment	green	225

T2-1	50.00	478	fiber	transparent	335
		479	fiber	transparent	3160
		480	fragment	transparent	1230
		481	fiber	transparent	1160
		482	fiber	transparent	345
		483	fiber	transparent	497
T2-2	50.15	484	fiber	transparent	621
		485	fiber	transparent	1870
		486	fiber	transparent	671
T3-1	50.00	487	fiber	transparent	836
		488	fiber	transparent	520
		489	fiber	transparent	1170
		490	fiber	blue	773
T3-2	50.01	491	fiber	other	497
		492	fiber	black	243
		493	pellet	black	79
		494	fiber	black	563
		495	fragment	blue	791
		496	fiber	blue	596
		497	fiber	black	372
		498	fiber	transparent	1130
T4-1	50.00	499	fiber	transparent	442
		500	fiber	blue	1240
		501	fiber	black	2680
		502	fiber	transparent	1580
		503	fiber	transparent	883
T4-2	50.13	504	fiber	green	1100
		505	fiber	transparent	926
		506	fiber	transparent	1450
		507	fiber	transparent	404
T5-1	50.13	508	fiber	blue	150
		509	fiber	transparent	2910
		510	fiber	black	659
		511	fiber	blue	552
		512	fiber	red	238
T5-2	50.23	513	fiber	blue	1210
		514	fiber	blue	1360

		515	fiber	transparent	729
		516	fiber	blue	481
		517	fiber	transparent	808
		518	fiber	transparent	1040
		519	fiber	green	1600
		520	fragment	blue	96
C1-1	50.10	521	fiber	transparent	1260
		522	fiber	transparent	1030
		523	fiber	blue	4010
		524	fiber	blue	224
C1-2	50.20	525	fiber	transparent	1510
		526	fragment	transparent	287
C2-1	50.15	527	fiber	transparent	1150
		528	fiber	transparent	1150
C2-2	50.42	529	fiber	blue	3140
		530	fiber	blue	1290
		531	fiber	blue	810
		532	fiber	red	284
		533	fiber	transparent	612
		534	fiber	blue	678
		535	fiber	transparent	1850
C3-1	50.28	536	fiber	blue	1840
		537	fragment	green	193
		538	fiber	blue	288
C3-2	50.05	539	fiber	transparent	1200
		540	fragment	blue	238
		541	fiber	blue	1070
C4-1	50.25	542	fragment	blue	92
		543	fiber	blue	115
		544	fragment	blue	127
		545	fiber	blue	210
		546	fiber	green	453
		547	fiber	blue	484
C4-2	50.15	548	fragment	transparent	517
		549	fiber	transparent	1270
		550	fiber	transparent	1430

References

Abidli, S., Toumi, H., Lahbib, Y., Trigui El Menif, N., 2017. The First Evaluation of Microplastics in Sediments from the Complex Lagoon-Channel of Bizerte (Northern Tunisia). *Water, Air, Soil Pollut*. 228.

Adams JK, Dean BY, Athey SN, Jantunen LM, Bernstein S, Stern G, et al. Anthropogenic particles (including microfibers and microplastics) in marine sediments of the Canadian Arctic. Science of the Total Environment 2021; 784

Baldwin, A.K., Spanjer, A.R., Rosen, M.R., Thom, T., 2020. Microplastics in Lake Mead National Recreation Area, USA: Occurrence and biological uptake. *Plos One* 15.

Ballent, A., Corcoran, P.L., Madden, O., Helm, P.A., Longstaffe, F.J., 2016. Sources and sinks of microplastics in Canadian Lake Ontario nearshore, tributary and beach sediments. *Mar. Pollut. Bull.* 110, 383-395.

Bharath, K.M., S, S., Natesan, U., Ayyamperumal, R., Kalam, S.N., S, A., K, S., C, A., 2021. Microplastics as an emerging threat to the freshwater ecosystems of Veeranam lake in south India: A multidimensional approach. *Chemosphere* 264, 128502.

Cincinelli, A., Scopetani, C., Chelazzi, D., Martellini, T., Pogojeva, M., Slobodnik, J., 2021. Microplastics in the Black Sea sediments. *Sci. Tot. Environ.* 760, 143898.

Dean, B.Y., Corcoran, P.L., Helm, P.A., 2018. Factors influencing microplastic abundances in nearshore, tributary and beach sediments along the Ontario shoreline of Lake Erie. 44, 1002-1009.

Felismino, M.E.L., Helm, P.A., Rochman, C.M., 2021. Microplastic and other anthropogenic microparticles in water and sediments of Lake Simcoe. *J. Great Lakes Res.* 47, 180-189.

Fischer, E.K., Paglialonga, L., Czech, E., Tamminga, M., 2016. Microplastic pollution in lakes and lake shoreline sediments - A case study on Lake Bolsena and Lake Chiusi (central Italy). *Environ. Pollut*. 213, 648-657.

Gopinath, K., Seshachalam, S., Neelavannan, K., Anburaj, V., Rachel, M., Ravi, S., Bharath, M., Achyuthan, H., 2020. Quantification of microplastic in Red Hills Lake of Chennai city, Tamil Nadu, India. *Environ. Sci. Pollut. Res. Int*. 27, 33297-33306.

Hu, D., Zhang, Y., Shen, M., 2020. Investigation on microplastic pollution of Dongting Lake and its affiliated rivers. *Mar. Pollut. Bull.* 160, 111555.

Masura, J., J. Baker, G. Foster, Courtney, A., 2015. Laboratory Methods for the Analysis of Microplastics in the Marine Environment: Recommendations for Quantifying Synthetic Particles in Waters and Sediments. NOAA Tech Memo. NOS-OR&R-4, 39.

Jiang, C., Yin, L., Wen, X., Du, C., Wu, L., Long, Y., Liu, Y., Ma, Y., Yin, Q., Zhou, Z., Pan, H., 2018. Microplastics in Sediment and Surface Water of West Dongting Lake and South Dongting Lake: Abundance, Source and Composition. *Int. J. Environ. Res. Public. Health.* 15.

Li, L., Geng, S., Wu, C., Song, K., Sun, F., Visvanathan, C., Xie, F., Wang, Q., 2019. Microplastics contamination in different trophic state lakes along the middle and lower reaches of Yangtze River Basin. *Environ. Pollut.* 254, 112951.

Liang, T., Lei, Z., Fuad, M.T.I., Wang, Q., Sun, S., Fang, J.K., Liu, X., 2021. Distribution and potential sources of microplastics in sediments in remote lakes of Tibet, China. *Sci. Total. Environ*. 806, 150526.

Liu, Y., Fang, J., 2020. Coastal Lakes as a Buffer Zone for the Accumulation and Redistribution of Plastic Particles from Continental to Marine Environment: A Case Study of the Dishui Lake in Shanghai, China. *Appl. Sci.* 10.

Mao, R., Song, J., Yan, P., Ouyang, Z., Wu, R., Liu, S., Guo, X., 2021. Horizontal and vertical distribution of microplastics in the Wuliangsuhai Lake sediment, northern China. *Sci. Tot. Environ.* 754.

Oni, B.A., Ayeni, A.O., Agboola, O., Oguntade, T., Obanla, O., 2020. Comparing microplastics contaminants in (dry and raining) seasons for Ox- Bow Lake in Yenagoa, Nigeria. *Ecotoxicol. Environ. Saf.* 198, 110656.

Scopetani, C., Chelazzi, D., Cincinelli, A., Esterhuizen-Londt, M., 2019. Assessment of microplastic pollution: occurrence and characterisation in Vesijarvi lake and Pikku Vesijarvi pond, Finland. *Environ. Monit. Assess*. 191, 652.

Sruthy, S., Ramasamy, E.V., 2017. Microplastic pollution in Vembanad Lake, Kerala, India: The first report of microplastics in lake and estuarine sediments in India. *Environ. Pollut.* 222, 315-322.

Turner, S., Horton, A.A., Rose, N.L., Hall, C., 2019. A temporal sediment record of microplastics in an urban lake, London, UK. *J. Paleol.* 61, 449-462.

Wen, X., Du, C., Xu, P., Zeng, G., Huang, D., Yin, L., Yin, Q., Hu, L., Wan, J., Zhang, J., Tan, S., Deng, R., 2018. Microplastic pollution in surface sediments of urban water areas in Changsha, China: Abundance, composition, surface textures. *Mar. Pollut. Bull.* 136, 414-423.

Yin, L., Wen, X., Du, C., Jiang, J., Wu, L., Zhang, Y., Hu, Z., Hu, S., Feng, Z., Zhou, Z., Long, Y., Gu, Q., 2020. Comparison of the abundance of microplastics between rural and urban areas: A case study from East Dongting Lake. *Chemosphere* 244, 125486.

Yin, L., Wen, X., Huang, D., Zeng, G., Deng, R., Liu, R., Zhou, Z., Tao, J., Xiao, R., Pan, H., 2021. Microplastics retention by reeds in freshwater environment. *Sci. Total. Environ.* 790, 148200.

Yuan, W., Liu, X., Wang, W., Di, M., Wang, J., 2019. Microplastic abundance, distribution and composition in water, sediments, and wild fish from Poyang Lake, China. *Ecotoxicol. Environ. Saf.* 170, 180-187.

Zhang, Q., Liu, T., Liu, L., Fan, Y., Rao, W., Zheng, J., Qian, X., 2021. Distribution and sedimentation of microplastics in Taihu Lake. *Sci. Total. Environ.* 795, 148745.

Zobkov, M., Belkina, N., Kovalevski, V., Zobkova, M., Efremova, T., Galakhina, N., 2020. Microplastic abundance and accumulation behavior in Lake Onego sediments: a journey from the river mouth to pelagic waters of the large boreal lake. *J. Environ. Chem. Engineer.* 8.